



**HAL**  
open science

## **Total Organic Carbon Evaluation Using Geophysical Well-Logs in Lorraine Coal Basin (NE France).**

Salim Allouti, Raymond Michels, Metzger Mombo Mouketo, Fabrice Malartre, Alain Izart, Yves Géraud, Vitaliy Privalov, Fady Nassif, Jacques Pironon, Philippe de Donato

### **► To cite this version:**

Salim Allouti, Raymond Michels, Metzger Mombo Mouketo, Fabrice Malartre, Alain Izart, et al.. Total Organic Carbon Evaluation Using Geophysical Well-Logs in Lorraine Coal Basin (NE France).. Bulletin de la Société Géologique de France, 2025, pp.1-53. <10.1051/bsgf/2025022>. <hal-05355466>

**HAL Id: hal-05355466**

**<https://hal.univ-lorraine.fr/hal-05355466v1>**

Submitted on 8 Nov 2025

**HAL** is a multi-disciplinary open access archive for the deposit and dissemination of scientific research documents, whether they are published or not. The documents may come from teaching and research institutions in France or abroad, or from public or private research centers.

L'archive ouverte pluridisciplinaire **HAL**, est destinée au dépôt et à la diffusion de documents scientifiques de niveau recherche, publiés ou non, émanant des établissements d'enseignement et de recherche français ou étrangers, des laboratoires publics ou privés.



Distributed under a Creative Commons CC BY 4.0 - Attribution - International License

# 1 Total Organic Carbon Evaluation Using Geophysical Well- 2 Logs in Lorraine Coal Basin (NE France).

3 Salim Allouti<sup>1\*</sup>, Raymond Michels<sup>1</sup>, Metzger Mombo Mouketo<sup>1</sup>, Fabrice Malartre<sup>1</sup>, Alain Izart<sup>1</sup>,  
4 Yves Géraud<sup>1</sup>, Vitaliy Privalov<sup>1,2</sup>, Fady Nassif<sup>3</sup>, Jacques Pironon<sup>1</sup>, Philippe de Donato<sup>1</sup>.

5  
6 <sup>1</sup> CNRS, GeoRessources Lab, Université de Lorraine, BP 70239, F-54506 Vandoeuvre-lès-Nancy, France

7 <sup>2</sup> M.P. Semenenko Institute of Geochemistry, Mineralogy and Ore Formation of the National Academy of Sciences of  
8 Ukraine, Kyiv, Ukraine

9 <sup>3</sup>La Française de l'Energie, Avenue du District, 57380 Pontpierre

10

11 *Author address: salim.allouti@univ-lorraine.fr*

## 12 **Abstract**

13 The Lorraine Coal Basin, recognized as the most promising coal bed methane basin in France,  
14 holds significance for the energy transition after more than a century of coal mining until 2004 and  
15 renewed interest in oil and gas exploration in the 80s and 90s. New data from an ongoing  
16 exploration campaign within this basin rise new opportunities in the assessment of gas resources.  
17 In the scope of this evaluation the determination of Total Organic Carbon (TOC) content using  
18 well-log data is a necessary step. The study employs a methodology encompassing Schmoker's  
19 method,  $\Delta\log R$ , and multivariate regression, focusing on two reference boreholes. While TOC  
20 calculations techniques are usually developed for marine shale deposits, an adaptation to highly  
21 heterogeneous fluvial deposits is presented. Schmoker's method provides the most accurate TOC  
22 values, consistent with Rock-Eval data. However, the  $\Delta\log R$  method underestimates TOC values,  
23 particularly for coal lithologies, for which logarithmic equations are proposed for proportional  
24 corrections. Moreover, new equations based on multivariate regression of gamma-ray, sonic, and

25 resistivity logs are developed for TOC estimation. Schmoker's method proves to be the most  
26 reliable with available density logs in the Lorraine Coal Basin. Alternatively, the modified  $\Delta \log R$   
27 equations or those derived from the multivariate regression of gamma-ray, sonic, and resistivity  
28 logs can be used. These new equations represent an alternative approach and identify new  
29 possibilities for estimating TOC in heterogeneous coaly formations. Based on TOC, lithologies of  
30 the investigated sedimentary series are classified from lean to fair source-rocks for shaly lithologies  
31 to excellent for the coal layer.

## 32 **Keywords**

33 Total Organic Carbon, Lorraine Carboniferous Basin, Coal Bed Methane, Well log,  $\Delta \log R$ ,  
34 Schmoker Method

35 **Résumé – Evaluation des teneurs en carbone organique total par les diagraphies dans le bassin**  
36 **carbonifère lorrain.** Le bassin carbonifère lorrain, reconnu comme l'un des bassins les plus  
37 prometteurs en France pour ses ressources en gaz de charbon (Coal Bed Methane - CBM), revêt  
38 une importance particulière pour la transition énergétique après plus d'un siècle d'exploitation  
39 charbonnière achevée en 2004 et un regain d'intérêt pour l'exploration pétrolière et gazière dans les  
40 années 1980 et 1990. De nouvelles données issues d'une campagne d'exploration en cours dans ce  
41 bassin facilitent l'évaluation des ressources gazières piégées dans les dépôts sédimentaires. Cette  
42 évaluation est réalisée en déterminant le Carbone Organique Total (COT) le long des puits, à l'aide  
43 des données diagraphiques. Plusieurs méthodes dans la littérature décrivent l'utilisation de la  
44 diagraphie dans le contexte des séquences marines, mais peu d'études se concentrent sur leur  
45 utilisation dans le cadre des dépôts continentaux. L'étude emploie une méthodologie englobant la  
46 méthode de Schmoker, la méthode  $\Delta \log R$ , et la régression multivariable, se concentrant sur deux

47 forages de référence : Fols 1A et Dbl S1. La méthode de Schmoker fournit les valeurs de COT les  
48 plus précises, cohérentes avec les données Rock-Eval. Cependant, la méthode  $\Delta\log R$  sous-estime  
49 les valeurs de COT, en particulier pour les lithologies charbonneuses, pour lesquelles des équations  
50 logarithmiques sont proposées afin de corriger ces estimations. De plus, de nouvelles équations  
51 basées sur la régression multivariable des logs gamma-ray, soniques et de résistivité sont  
52 développées pour l'estimation du COT. La méthode de Schmoker s'avère être la plus fiable avec  
53 les logs de densité disponibles dans le bassin houiller lorrain. Alternativement, les équations  $\Delta\log R$   
54 modifiées ou celles dérivées de la régression multivariable des logs gamma-ray, soniques et de  
55 résistivité peuvent être utilisées. Ces nouvelles équations peuvent constituer une approche  
56 innovante et ouvrir des pistes à explorer pour estimer le TOC dans les niveaux riches en matière  
57 organique. Sur la base du COT, les lithologies des séries sédimentaires étudiées peuvent être  
58 classées de roches mères pauvres à moyennes pour les lithologies argileuses, et excellentes pour  
59 les couches de charbon.

## 60 **Mots clés**

61 Carbone organique total, Bassin carbonifère lorrain, Gaz de charbon, Diagraphie,  $\Delta\log R$ ,  
62 Méthode de Schmoker.

## 63 **1. Introduction**

64 After more than a century of coal exploitation until 2004 and exploration for oil and gas during the  
65 80s-90s, renewed interest in evaluating of the gas reserves of the Lorraine Carboniferous basin has  
66 emerged in recent years ([Gunzburger, 2019](#)). Currently, the Lorraine Basin is undergoing a new  
67 investigation, with recent drillings providing both core and well log data. Previous studies  
68 described the coal seams distribution ([Donsimoni, 1981](#)), the organic geochemistry of coal and

69 kerogen-bearing strata ([Fleck, 2001](#)), reconstructed the burial history of the basin, and evaluated  
70 gas generation ([Izart et al., 2016](#)). However, until recently no attempt was made to quantitatively  
71 evaluate the gas generation potential of the basin as part of the assessment of the ultimate gas  
72 reserves.

73 The Total Organic Carbon content (TOC) is a key parameter to assess the gas potential of  
74 sedimentary strata ([Passey et al., 1990](#)). While major coal strata are well characterized in the  
75 Lorraine basin wells, the quantitative estimation of the abundance of kerogen present in  
76 surrounding rock facies (clay, siltstone, sandstone, and conglomerate) has never been evaluated in  
77 a continuous manner along the formations, as previous studies ([Fleck, 2001](#)) relied on sampling  
78 approaches that did not capture the full complexity. Yet, the calculation of the total gas generation  
79 potential of the Carboniferous deposits requires the appraisal of all organic matter-containing  
80 facies.

81 TOC measurements in the laboratory may be performed by carbon analyzers ([Van Krevelen, 1993](#))  
82 or Rock-Eval pyrolysis ([Espitalié et al., 1985](#)) applied to core samples and drilling cuts. However,  
83 these laboratory measurements are time-consuming and the TOC data is discontinuously  
84 determined along the sedimentary profiles. To overcome this drawback, methods involving well-  
85 logging methods have been developed to assess TOC contents.

86 Well-logging techniques have greatly enhanced the exploration of Coalbed Methane (CBM)  
87 reservoirs by providing workflows to evaluate coal quality, and reservoir parameters such as  
88 fracture density, permeability, and gas content ([Morin, 2005](#); [Chatterjee and Paul, 2013](#); [Meng et](#)  
89 [al., 2013](#); [Sutton et al., 2014](#); [Ghosh et al., 2016](#); [Su et al., 2018](#)).

90 The systematic determination of the TOC content of sedimentary logs by such methods has  
91 however mostly been developed for marine petroleum source rocks ([Nixon, 1973](#); [Meissner, 1987](#);  
92 [Meyer and Nederlof, 1984](#); [Mendelzon and Toksoz, 1985](#); [Mann and Muller, 1986,1988](#); [Passey et](#)  
93 [al., 1990](#) ; [Bessereau et al., 1991](#);[Schwarzkopf., 1992](#)).

94 [Schmoker \(1979, 1981\)](#) first published a method to calculate TOC content from density and  
95 gamma-Ray logs. [Schmoker \(1979\)](#) proposed a linear relationship between TOC and the formation  
96 density log in shales. Generally, shale mineral matrix density presents an average value of  
97  $2.7 \text{ g/cm}^3$  while matrix density values for organic matter are approximately  $1.1 \text{ g/cm}^3$ . The  
98 occurrence of organic carbon vastly influences the formation bulk density and hereafter TOC is  
99 calculated from density logs. [Meyer and Nederlof \(1984\)](#) and [Mendelzon and Toksoz \(1985\)](#) used  
100 a combination of density, sonic slowness, and electrical resistivity logs to calculate Total Organic  
101 Carbon (TOC) for characterizing petroleum systems. They explained that source rocks are  
102 characterized by their low density, low sonic slowness, and high electrical resistivity. To improve  
103 TOC assessment, [Passey et al. \(1990\)](#) proposed to use a combination of well-logs and developed  
104 the  $\Delta\log R$  technique, which consists of the overlay of porosity (sonic, density, neutron) with  
105 resistivity logs. In organic matter-rich sediments, the two geophysical signals exhibit distinct  
106 characteristics, and the magnitude of their separation is primarily proportional to TOC, with  
107 additional influence from the thermal maturity of the formation (including the presence of oil and  
108 gas). Consequently, utilization charts have been developed based on vitrinite reflectance to account  
109 for these factors. This method has limitations in terms of accuracy for interwell correlation, as the  
110  $\Delta\log R$  technique requires the arbitrary selection of a baseline, which varies significantly from well  
111 to well due to lithological variations ([Yu et al., 2017](#); [Wang, 2022](#)) and thermal maturity of kerogen  
112 ([Sun et al., 2013](#)). In fact, the thermal maturity of the formations intersected by the wells can

113 influence the porosity, which is susceptible to measurement by density, sonic, and resistivity logs,  
114 thereby leading to variations in the log readings between wells.

115 In shale and coal, the  $\Delta\log R$  method requires calibration as it tends to underestimate the Total  
116 Organic Carbon content in these formations ([Sondergeld et al., 2010](#)). To address this, alternative  
117 approaches are proposed to determine correction coefficients in organic-rich layers ([Sondergeld et](#)  
118 [al., 2010](#)). Additionally, the inclusion of other well logs, such as natural gamma spectroscopy, is  
119 proposed by [Li and Zhang \(2023\)](#).

120 [Bessereau et al. \(1991\)](#) introduced the CARBOLOG method, which utilizes Sonic slowness and  
121 resistivity well logs taking into account the composition of rock, including matrix, water, clay, and  
122 organic matter. The method defines the CARBOLOG diagram, where the square root of resistivity  
123 is plotted against sonic slowness.

124 Moreover, statistical methods, such as multivariate analyses, are employed to predict TOC,  
125 demonstrating good correlations between density logs and the predicted TOC ([Zhang and Xu,](#)  
126 [2016; Nyakilla et al., 2022](#)). However, the generalization of these models is not possible for all  
127 continental shales and coal due to weak linear correlations with log curves ([Hu et al., 2016; Wang](#)  
128 [et al., 2017](#)). Currently, the most advanced method for calculating Total Organic Carbon (TOC)  
129 utilizing well-log data is the application of machine learning algorithms ([Huang and Williamson,](#)  
130 [1996; Kamali and Mirshady, 2004; Amiri Bakhtiar et al., 2011; Khoshnoodkia et al., 2011;](#)  
131 [Alizadeh et al., 2012; Cranganu and Dimitrijevic , 2016; Bolandi et al., 2017; Mahmoud et al.,](#)  
132 [2017, 2019; Nezhad et al., 2018; Wang et al., 2018; Zhu et al., 2018; Elkatatny, 2019; Zhao, 2019;](#)  
133 [Goliatt and Saporetti, 2023; Zhu et al., 2023; Wood, 2023](#)). However, there is currently no  
134 standardized algorithm established for the computation of TOC from well logs. This limitation can

135 be primarily attributed to the heterogeneity of lithological formations ([Chan et al., 2022](#)). [Passey](#)  
136 [et al. \(1990\)](#) had already noted that TOC values obtained using their approach were unreliable for  
137 organic matter-rich layers with thicknesses less than 1 meter. However, a significant challenge  
138 arises from the complexity of sedimentary successions, particularly in continental detrital deposits.  
139 This is the case for instance for the fluvial facies which are dominant in the Lorraine Carboniferous  
140 Basin and characterized by hundreds of fining upward depositional sequences (conglomerate to  
141 sandstone, silt, clay, and coal seams). Therefore, this study aims to calculate Total Organic Carbon  
142 (TOC) using well logs across all fluvial-lacustrine sedimentary facies, contributing to the gas  
143 reserve calculations.

## 144 **2. Geological setting**

145 The Lorraine Carboniferous Basin, located in North-East France, is about 200 km long and 80 km  
146 wide. It extends into the German Saar-Nahe Basin where strata outcrop ([Schäfer, 2011](#)) ([Fig. 1](#)).  
147 In the French part, the basin is bounded to the north by the Metz-Hunsrück Fault, a major SW-NE  
148 trending thrust fault belonging to Variscan orogeny ([Henk, 1993](#); [Schäfer, 2005](#), [Hemelsdaël et al.,](#)  
149 [2023](#)), to the south by the gravity anomaly between Sarrebourg and Gironcourt and to the west by  
150 La Marne Fault ([Donsimoni, 1981](#); [Izart et al., 2016](#)). It is an intermountain basin (Courel et al.,  
151 1986; Donsimoni, 1981; [Hemelsdaël et al., 2023](#)) that developed during the Hercynian orogeny  
152 and therefore contains no marine sediments ([Schäfer, 1989, 2005, 2011](#)). More precisely, the  
153 Lorraine Carboniferous basin developed during the compression phase and late collapse phase of  
154 the Variscan belt. The main part of the sedimentary filling consists of up to 8 km of Westphalian-  
155 Stephanian detrital sediments covered by Permian and Mesozoic deposits of about 500 m thickness  
156 on average ([Pruvost, 1934](#); [Donsimoni, 1981](#); [Barrabé and Feys, 1965](#); [Izart et al., 2016](#)).

157 In this study, well logs investigated stratigraphical interval is comprised between the top of  
158 Westphalian C to top Westphalian D. Those regional lithostratigraphical and biostratigraphical  
159 subdivisions can be correlated to the international chronostratigraphical chart ([Gradstein et al.,](#)  
160 [2020](#)), and assigned to Middle and Late Pennsylvanian stages, thanks to the datings of zircons from  
161 the volcanic tuffs of the Saar and Lorraine basins ([Izart et al., 2025](#)). These authors dated the  
162 Westphalian B/Westphalian C boundary (313.82 Ma), the mid-part of the Westphalian C (313.24  
163 Ma), the Westphalian D top (307.95 Ma) and the Early Stephanian (304.49 Ma), and proposed a  
164 correlation with the other regional substages from the Western European coal basins. The  
165 Westphalian B corresponds to the Duckmantian regional substage, the Westphalian C to the  
166 Bolsovian, the Westphalian D to the Asturian, and the Early Stephanian to the upper part of the  
167 Cantabrian and Barruelian. The marine global stages corresponding to these local substages are  
168 respectively the Moscovian and the Kasimovian, assigned to the Middle and Late Pennsylvanian.

169 At the basin scale, the sedimentary deposits are subdivided into two major series which were  
170 defined essentially by palynological and paleobotanical data in galleries and boreholes ([Pruvost,](#)  
171 [1934](#); [Laveine, 1974](#); [Alpern et al., 1969](#); [Termier, 1923](#); [Merry, 1967](#); ([Izart et al., 2025](#)): i) The  
172 Westphalian series displaying approximately 4 km of accumulated deposits with about a hundred  
173 coal beds. Their thickness varies from a few centimeters to a maximum of 25 meters exceptionally,  
174 with an average of four to five meters. ii) The Stephanian series of about 1.1 km of deposits  
175 containing four major coal layers.

176 Coal layers are interstratified within all grain size siliciclastic series with variable thicknesses of  
177 conglomerates, sandstones, siltstones, and claystones. Deposits show differential preservation due  
178 to the development of recurrent erosional surfaces.

179 A wide spectrum of different continental environments ([figs. 2 and 3](#)), studied by [Izart et al. \(2005\)](#)  
180 for the Westphalian C and [Allouti \(2024\)](#) for the Westphalian D, can be highlighted, with from  
181 source to sink restricted to that intermountain context, alluvial fans, braided rivers, meandering  
182 rivers, anastomosed rivers with more or less preserved floodplains, and finally delta-lakes where  
183 sediment storage become permanent due to provided suitable accommodation. River systems were  
184 interconnected to well-developed lowland swamps and lakes organized in variable continuous  
185 areas with rich and diversified plant life induced high organic productivity ([Pruvost, 1934](#);  
186 [Donsimoni, 1981](#); [Fleck et al., 2001](#); [Izart et al., 2005](#)). Higher proportion of floodplain deposits  
187 give appropriate conditions to more widespread distribution of coal. Moreover, organic-rich  
188 swamps were to show rapid rate of organic growth and accumulation outpaces clastic  
189 sedimentation. This kind of sedimentological evolution and stratigraphical organization is typical  
190 of depositional environments for Carboniferous coal-bearing strata ([McCabe, 1985](#); [Diessel, 1992](#);  
191 [Thomas, 2002](#)). The high frequency sequences reported in the figures 2 and 3 were determined by  
192 [Allouti \(2024\)](#) and their durations (close to 20 ka, precession-scale) were calculated by [Izart et al.](#)  
193 [\(2025, their Fig. 5\)](#) thanks to the Bayesian method.

### 194 **3. Materials and Methods**

#### 195 **3.1. Data availability**

##### 196 **3.1.1. Studied wells and core samples**

197 The study is focused on two boreholes, Folschviller (Fols 1A) and Diebling (Dbl S1), which were  
198 drilled by La Française de l'Energie company and penetrated the top of the Carboniferous units  
199 ([Figs. 1, 2 and 3](#)). Fols 1A reached Westphalian D in the (690-1303 m TVD interval), while Dbl S1  
200 drilled through Westphalian D (875-1265 mTVD interval) and Westphalian C (1265-1440 m TVD

201 interval). Detailed lithologies, depositional environments as well as stratigraphic sequences are  
202 synthesized in Figures 2 and 3. Thirty-seven samples were collected from these boreholes,  
203 including coals and shaly coals, claystones, siltstones, and sandstones.

### 204 **3.1.2. Organic petrography and Rock-Eval analysis**

205 The rock and coal samples were crushed, sieved (<180 µm mesh), and analyzed by Rock-Eval  
206 pyrolysis at the Institut des Sciences de la Terre d'Orléans (ISTO) (France) (analytical procedure  
207 described in [Le Meur et al. \(2021\)](#)). The major parameters considered were TOC (wt%) and  
208 Tmax (°C). Organic petrography and vitrinite reflectance measurements were assessed by EGS-  
209 exploration (Switzerland).

### 210 **3.1.3. Well logs data**

211 The well logs are presented in Log Ascii Standard (LAS) format for both the boreholes Fols 1A  
212 and Dbl S1. Data were imported into Techlog© Schlumberger software and then exported to  
213 Microsoft Excel© to evaluate TOC using  $\Delta$ logR and Schmoker methods. Gamma-Ray, Sonic, and  
214 Density Logs are used to determine shale volume, total porosity, and lithological interpretation.  
215 TOC computation involves Sonic, Density, and Resistivity Logs. The caliper is also available for  
216 both wells to control potential washout/breakout detected by borehole diameter widening in some  
217 coal layers.

## 218 **3.2 Methods of Calculating Total Organic Carbon Using Well-Logs**

### 219 **3.2.1. Well Log Responses for Characterizing Coal Deposits**

220 Various methods for identifying and characterizing coal layers and organic-rich strata in subsurface  
221 rock units, including gamma-ray, density, resistivity, sonic slowness, and caliper measurements are  
222 described in the literature ([Seidle, 2011](#); [Keskinsezer et al., 2019](#); [Thomas, 2002](#)).

223 The gamma-ray method involves measuring the intensity of naturally occurring gamma rays. Coal  
224 layers typically exhibit low gamma ray values, whereas clayey formations present high values.  
225 Also, gamma ray values are lower in lithologies such as sandstones and conglomerates ([Hollub and  
226 Schafer, 1992](#); [Karacan, 2009](#); [Seidle, 2011](#); [Keskinsezer et al., 2019](#)). Therefore, this tool cannot  
227 be used alone to identify organic-rich sediments.

228 In regards to the use of density logs, coal and organic-rich strata typically exhibit lower density  
229 values compared to other lithologies ([Mavor et al., 1994](#); [Zhou and Esterle, 2008](#); [Keskinsezer et  
230 al., 2019](#)).

231 In terms of resistivity, coal layers exhibit higher values, but only when the water content is low  
232 ([Keskinsezer et al., 2019](#)). The resistivity of coal is dependent on its rank, with lignite and  
233 anthracite displaying very low resistivity and subbituminous and bituminous coal displaying a  
234 range from low to high resistivity values ([Mavor et al., 1994](#); [Thomas, 2002](#)). In addition, resistivity  
235 may be influenced by factors such as water saturation and salinity as well as quantity of clay or  
236 conductive minerals like pyrite ([Sondergeld et al., 2010](#)) and must therefore be combined with  
237 other tools to determine the organic matter content of strata.

238 Sonic logs are valuable tools for identifying coal layers ([Rider and Kennedy, 2011](#); [Seidle, 2011](#)).  
239 The sonic wave transit time in coal range generally between those of sandstone and shale. However,  
240 anthracite coal, with a transit time of approximately 90  $\mu\text{s}/\text{ft}$ , exhibits a response closely resembling  
241 that of shale, making accurate discrimination more challenging. While sonic logs are useful in

242 assessing coal quality, their application to coal gas reservoir engineering is limited by certain  
243 constraints such as breakout and washout. Nonetheless, sonic logs combined with the previously  
244 mentioned tools may serve as indicators of organic matter content ([Passey et al., 1990](#); [Meyer and](#)  
245 [Nederlof, 1984](#)).

246 The caliper log is used for measuring the diameter of the borehole and serves as an effective quality  
247 control for other wireline logs, including density, gamma-ray, and sonic logs. By applying this tool,  
248 errors in the identification of coal layers caused by unusually low formation density and gamma  
249 ray responses across severe washouts can be prevented. It should be noted that while washout is  
250 often considered an indicator of permeability, as well as an indicator of coal mechanical friability  
251 ([Thomas, 2002](#)).

### 252 **3.2.2. Schmoker Method**

253 [Schmoker \(1979\)](#) developed a method for estimating TOC contents of Appalachian Devonian  
254 marine shale using a density log RHOb. [Schmoker and Hester \(1983\)](#) suggested that TOC has a  
255 positive linear correlation with the reciprocal of bulk density:

$$\text{TOC} = \frac{A}{\text{RHOb}} - B \quad (1)$$

256 [Schmoker \(1979, 1981\)](#) considered the rock is composed of mineral matrix, interstitial pores,  
257 pyrite, and organic matter. In this case, the formation bulk density is a function of fractional  
258 densities and volumes of these four components. The volume of pyrite was assumed to increase  
259 linearly with the organic matter content because the decomposition of organic matter generates  
260 reducing conditions that promote pyrite formation in anoxic environments. For this reason, pyrite

261 was treated as a separate component from the matrix. The values of A and B in equation (1) are  
 262 calculated by incorporating density values for pyrite, organic matter, and matrix at 5.0, 1.01, and  
 263 2.69 g/cm<sup>3</sup>, respectively.

$$\text{TOC} = \frac{154.497}{\text{RHOb}} - 57.261 \quad (2)$$

### 264 3.2.3. $\Delta \log R$ Method

265 [Passey et al. \(1990\)](#) proposed  $\Delta \log R$  method for estimating TOC content from well-log data.  
 266 Currently, the  $\Delta \log R$  is a widely used method for marine clay series. The  $\Delta \log R$  technique requires  
 267 the superposition of resistivity with porosities logs (sonic slowness  $\Delta T$ , density RHOb or neutron  
 268 porosity  $\Phi_n$ ; in equations 3, 4 and 5) and the availability of organic matter maturity data (e.g.  
 269 vitrinite reflectance). The integration of sonic slowness and resistivity logs facilitates the  
 270 identification of a baseline cutoff. A distinct separation between the two curves indicates the  
 271 presence of source rock zones, while the overlap of the curves signifies non-source rock intervals.  
 272 (Fig. 4).

$$\Delta \log R = \log_{10} \left( \frac{R}{R_{\text{Baseline}}} \right) + 0.02 * (\Delta t - \Delta t_{\text{Baseline}}) \quad (3)$$

$$\Delta \log R = \log_{10} \left( \frac{R}{R_{\text{Baseline}}} \right) + 4 * (\phi_t - \phi_{t_{\text{Baseline}}}) \quad (4)$$

$$\Delta \log R = \log_{10} \left( \frac{R}{R_{\text{Baseline}}} \right) - 2,5 * (\text{RHOb} - \text{RHOb}_{\text{Baseline}}) \quad (5)$$

273 In this study, equation (3) is used to calculate  $\Delta \log R$ . The amount of organic carbon is directly  
274 proportional to  $\Delta \log R$ , consequently, TOC can be calculated using equation (6).

$$\text{TOC} = \Delta \log R * 10^{(2.297-0.1688*\text{LOM})} \quad (6)$$

275 If the Level of Maturity (LOM) is known, the  $\Delta \log R$  separation of different lithologies using well  
276 logs data can be used to estimate the TOC. LOM is a scale of organic matter thermal evolution  
277 applicable to fine-grained sedimentary rocks proposed by [Hood \*et al.\* \(1975\)](#). LOM values were  
278 estimated from vitrinite reflectance (%Ro) values using equation (7).

$$\text{LOM} = 0.0989 \times \text{Ro}^5 - 2.1587 \times \text{Ro}^4 + 12.392 \times \text{Ro}^3 - 29.032 \times \text{Ro}^2 + 32.53 \times \text{Ro} - 3.0338 \quad (7)$$

279 Thermal maturity values for the Westphalian D formation in the Lorraine Carboniferous Basin,  
280 Fols 1A and Dbl S1 wells are available in [Table 1](#). The equation for LOM was determined from  
281 digitalization of the % Ro correlation table established by [Hood \*et al.\* \(1975\)](#).

## 282 **4. Results**

### 283 **4.1. TOC calculation using Schmoker**

284 The widely used TOC calculation method proposed by [Schmoker \(1979, 1981\)](#) is represented by  
285 equation (2) with constants A and B of 154.497 and 57.261 respectively. These values are not  
286 always suitable for any well and may thus be adjusted for our reference wells Fols 1A and Dbl S1.  
287 These constants are typically gauged from the linear regression of TOC Rock-Eval and density log  
288 ([Schmoker and Hester, 1983](#); [Yu \*et al.\*, 2017](#)).

289 In the case of the Fols 1A borehole the crossplots of the TOC Rock-Eval versus 1/density and TOC  
290 Schmoker versus TOC Rock-Eval (Fig. 5a and b) reveal a linear relationship that closely matches  
291 with equation (2) with acceptable correlation coefficients. In this case, correction of A and B may  
292 not be applied.

293 In the case of the borehole Dbl S1, the same graphs show significant deviations (Fig. 5) revealing  
294 that the A and B parameters of the original Schmoker method induce an underestimation of TOC  
295 values. Consequently, constants A and B are changed to 256.02 and 100.4 respectively for the  
296 Dbl S1 borehole (Fig. 5a; Eq. 8).

$$\text{TOC} = \frac{256.02}{\text{RHOb}} - 100.4 \quad (8)$$

297 Figure 5b shows the relationship obtained between Rock-Eval TOC and TOC calculated using the  
298 adapted Schmoker equation. The TOC values are calculated using the Schmoker relationship, and  
299 are used as a reference for the other developed relationship.

#### 300 **4.2. TOC calculation using $\Delta \log R$**

301 Continuous sonic and resistivity logs are available for the Fols 1A and Dbl S1 boreholes. Prior to  
302 overlaying the curves, appropriate scaling is necessary to ensure that each resistivity cycle  
303 corresponds to 50  $\mu\text{s}/\text{ft}$ . Following scaling, the curves require baseline definition. Baseline  
304 resistivity and sonic values are established at 150 ohm.m and 65  $\mu\text{s}/\text{ft}$  for the Fols 1A well and  
305 100 ohm.m and 80  $\mu\text{s}/\text{ft}$  for the Dbl S1 well (Tab. 2 and Fig. 4). Equation (3) is then used to  
306 calculate the  $\Delta \log R$  separation in this study (Fig. 4), which enables the estimation of TOC using  
307 equation (6).

308 For Fols 1A and Dbl S1 wells, TOC values were calculated by applying the  $\Delta\log R$  method and  
309 equal to 8 wt% for coal layers. These values are approximately ten-fold lower than the TOC values  
310 obtained from Rock-Eval analysis, which range from 20 to 75 wt% in Fols 1A and 10 to 85 wt%  
311 in Dbl S1, with maximum values of 75 and 85 wt%, respectively. For shaly lithologies, mean TOC  
312 values are 0.5 wt% in both wells, which is lower than the values obtained from Rock-Eval analysis  
313 in Fols 1A (7 wt% TOC on average) and Dbl S1 (3 wt% on average) (Track 2 in [Figs. 6 and 7](#)  
314 respectively).

### 315 **4.3. TOC calculation using Modified $\Delta\log R$ Method**

#### 316 **4.3.1. TOC Schmoker vs. TOC $\Delta\log R$ evaluation**

317 The Schmoker and calibrated Schmoker methods as defined above allow to calculate TOC values  
318 in good agreement with Rock Eval data measured on the various lithologies (coal, shaly coals,  
319 coaly shales, sandstones, conglomerates) present in our wells ([Figs. 6 and 7](#)). The Schmoker  
320 method may then be considered as the most appropriate for our study. In contrast, the  $\Delta\log R$   
321 method tends to underestimate TOC values for coaly and shaly lithologies. Cross-plot analyses  
322 using TOC Schmoker/ TOC  $\Delta\log R$  versus geophysical parameters (Sonic slowness, bulk density,  
323 and resistivity) are tested. Only the cross-plot using sonic slowness showed a consistent trend ([Fig.](#)  
324 [8a](#)) in which values greater than 80  $\mu\text{s}/\text{ft}$  and 100  $\mu\text{s}/\text{ft}$  for Fols 1A and Dbl S1 respectively  
325 represented a logarithmic trend with a convergence limit of 10. The consideration of bulk density  
326 (color scale ([Fig. 8a](#))) shows that these points correspond to low-density values related to coal and  
327 coaly facies. Changes in density values from 1.7 to 2.3  $\text{g}/\text{cm}^3$  correspond to increasing shale volume  
328 on carbonaceous lithologies. All data points showing sonic slowness values lower than 70  $\mu\text{s}/\text{ft}$  and

329 high density (more than 2.3 g/cm<sup>3</sup>) are related to non-source rock formations (sandstones and  
330 conglomerates) and displayed no correlation with sonic slowness.

331 The cut-off values of 80 μs/ft and 100 μs/ft were applied to select shale, shaly coal, and coal from  
332 [figure 8a](#). For coaly lithologies, the minimum sonic slowness value is 80 μs/ft for Fols 1A and  
333 100 μs/ft for Dbl S1, while the maximum value is 140 μs/ft for Fols 1A and 160 μs/ft for Dbl S1.  
334 The analysis of the data reveals a logarithmic increase in the ratio in relation to sonic slowness,  
335 ranging from 0.1 to 10 as shown in [figure 8b](#). Equations (9) and (10) represent this relationship for  
336 Fols 1A and Dbl S1 wells, respectively.

$$(\text{TOC Schmoker})/(\text{TOC } \Delta \log R) = 19.15 * \ln(\Delta T) - 83.48 \quad (9)$$

$$(\text{TOC Schmoker})/(\text{TOC } \Delta \log R) = 23.298 * \ln(\Delta T) - 101 \quad (10)$$

337 Therefore, to mitigate the discrepancy between TOC values calculated by ΔlogR and measured by  
338 Rock-Eval, equations (11) and (12) are applied as sonic slowness filters to wells Fols 1A and  
339 Dbl S1 respectively. Proportional corrections are thus applied to shaly and coaly lithologies while  
340 values for non-source rock formations are left unaltered.

$$\text{TOC} = \Delta \log R * 10^{(2.297-0.1688*\text{LOM})} * (19.15 * \ln(\Delta T) - 83.48) \quad (11)$$

$$\text{TOC} = \Delta \log R * 10^{(2.297-0.1688*\text{LOM})} * (23.298 * \ln(\Delta T) - 103.48) \quad (12)$$

341 [Figure 6](#) (track 8) and 6 (track 6) show the consistency between assessed and measured TOC values  
342 once the corrections are applied. The box plot ([Fig. 9](#)) for the Fols 1A borehole shows that upon

343 application of the logarithmic factor to the  $\Delta\log R$  method, 50 % of coal sample points analyzed  
344 exhibit TOC ranging from 30 wt% to 60 wt%. Also, 50 % of shaly lithology sample points  
345 analyzed exhibit an average TOC amount ranging from 3 wt% to 6 wt%. Similarly, after correction  
346 of the  $\Delta\log R$  method via the logarithmic factor, the box plot for the Dbl S1 borehole (Fig. 9)  
347 indicates that 50 % of coal sample points analyzed exhibit a TOC amount ranging from 20 wt% to  
348 70 wt%, with 50 % of shaly lithology sample points analyzed exhibiting an average TOC amount  
349 ranging from 3 wt% to 6 wt%.

#### 350 4.3.2. “ $\Delta$ . log R separation” and TOC calibration

351 In the method proposed by [Passey et al. \(1990\)](#), the relationship between TOC values and the  
352 separation  $\Delta\log R$  is given by equation (6), which requires the consideration of LOM (Level of  
353 Organic Maturity, a factor proportional to vitrinite reflectance) ([Hood et al., 1975](#)). The results for  
354 our sample sets (LOM=10.12 -10.65; %Ro = 0.84 to 0.96 and TOC as determined by Rock-Eval)  
355 are consistent with  $\Delta\log R$  method for facies with TOC lower than 10 wt%. However, for TOC  
356 greater than 10 wt%, the data points fall outside the range, indicating that equation (6) may not be  
357 appropriate for coaly facies (Fig. 10). These findings have important implications for the  
358 interpretation of well-log data, as they suggest that the linear LOM trends proposed by [Passey et](#)  
359 [al. \(1990\)](#) may not apply for coaly facies. Therefore, alternative equations may be proposed for  
360 TOC determination in coal-rich deposits. Two approaches are used to calibrate TOC values over a  
361 large range: i) Rock-Eval TOC (using the depth average where the sample was taken) and ii) TOC  
362 calculated using the method by [Schmoker \(1979, 1981\)](#) as validated previously vs  $\Delta \log R$ .

363 In figure 11 (borehole Fols 1A), two correlation equations may be derived from Rock-Eval TOC  
364 vs  $\Delta \log R$ , a polynomial (Eq. 13) (red solid line) and an exponential (Eq. 14) (red dashed line).

365 When considering TOC calculated after [Schmoker \(1979, 1981\)](#) and  $\Delta \log R$ , a polynomial  
366 (Eq. 15) (blue solid line) and an exponential (Eq. 16) (blue dashed line) are derived.

$$\text{TOC} = 22.117 * \Delta \log R^2 + 6.997 * \Delta \log R \quad (13)$$

$$\text{TOC} = e^{2.6136 * \Delta \log R} \quad (14)$$

$$\text{TOC} = 16.262 * \Delta \log R^2 + 6.5631 * \Delta \log R \quad (15)$$

$$\text{TOC} = e^{2.4374 * \Delta \log R} \quad (16)$$

367 In [Fig. 12](#) (borehole Dbl S1), a correlation between Rock-Eval TOC and  $\Delta \log R$  results in a  
368 polynomial (Eq. 17) (red solid line). Correlation between Schmoker TOC and  $\Delta \log R$  leads to a  
369 polynomial (Eq. 18) (blue solid line).

$$\text{TOC} = -8.5903 * \Delta \log R^2 + 64.702 * \Delta \log R - 12.655 \quad (17)$$

$$\text{TOC} = -3.2901 * \Delta \log R^2 + 45.123 * \Delta \log R - 2.4875 \quad (18)$$

#### 370 4.4. TOC calculation using Multivariate Regression

371 As the density log is not always available for all the wells of our basin, it is interesting to further  
372 explore the relationship between calculated TOC using [Schmoker \(1979, 1981\)](#) and various  
373 borehole logs. Therefore, we conducted multivariate regression analyses using gamma ray (GR),  
374 sonic ( $\Delta t$ ), and resistivity (R) logs in regard to TOC as determined by the Schmoker method

375 validated by TOC Rock-Eval. Based on a total of 8785 measurements for Fols 1A and 6381  
376 measurements for Dbl S1, the multivariable regression analysis led to the following equations:

$$\text{Fols 1A: TOC} = 0.73 * \Delta t - 0.065 * GR + 0.02 * R - 46.29 \quad (19)$$

$$\text{Dbl S1: TOC} = 0.82 * \Delta t - 0.066 * GR + 0.02 * R - 64.15 \quad (20)$$

377 With determination coefficient R2 of 0.82 and 0.73 respectively. This indicates a strong  
378 relationship between TOC and the geophysical variables (gamma ray, sonic, and resistivity logs)  
379 for both boreholes (Fig. 6 Track 7 and Fig. 7 Track 5).

## 380 5. Discussion

381 The analysis of logs signals in Fols 1A and Dbl S1 boreholes revealed discrepancies in the  
382 equations used to calculate TOC primarily due to sonic slowness value deviations of 20  $\mu\text{s}/\text{ft}$   
383 between the two boreholes. Fols 1A exhibits less dispersion around correlation curves and a higher  
384 correlation coefficient compared to Dbl S1. The divergence stems from contrasting sediment  
385 composition. The siltites, sandstones, and conglomerates from the Fols 1A borehole are litharenites  
386 rich in pseudo-detrital matrix with abundant micritic siderite cementation, while those from Dbl  
387 S1 are of better sorting (mineralogical and grain sized based sorting) with low pseudo-detrital  
388 matrix contribution and far less authigenic siderite. The predominant types of cement are later  
389 diagenetic phases such as dickite and illite. Furthermore, the burial history of the two boreholes  
390 varies. Fols 1A experienced greater burial and compaction due to its structural position on the flank  
391 of a syncline) compared to Dbl S1, which is positioned on the hinge zone of an anticline.

392 The application of the Schmoker method on this case study well-log data leads to TOC values that  
393 are consistent with those obtained from Rock-Eval measurements on rock samples. The Schmoker  
394 equation for TOC calculations considers the contribution of organic matter, pyrite, interstitial  
395 porosity, and rock matrix as variables. [Schmoker \(1979, 1981\)](#) demonstrated a proportional  
396 relationship between the abundance of organic matter and pyrite and integrated this into equation  
397 (1). Yet, his study was based on claystone deposited in the marine environment. It is well known  
398 that in the anoxic sulfate-rich marine waters, organic matter is a substrate for the growth of sulfate-  
399 reducing bacteria communities which generate reduced sulfur. In the presence of detrital minerals,  
400 reduced iron is combined with sulfur to produce iron sulfide, hence the relationship observed by  
401 [Schmoker \(1979, 1981\)](#). In this case study, sediments were deposited in a fluvial-lacustrine system  
402 without connection to the marine environment ([Donsimoni, 1981](#); [Izart et al., 2005](#); [Fleck et al.,](#)  
403 [2001](#)) and therefore poor in sulfate. As a consequence, the coal layer present is lean in pyrite.

404 As considered by [Schmoker \(1979, 1981\)](#), porosity may be considered as constant for a given facies  
405 (marine claystone in his study cases) and thus may not influence TOC calculation. In the present  
406 case study, regarding the diversity of facies from coal to conglomerate, the influence of porosity  
407 changes may be questioned. Conglomerate aside, the studied facies present porosities up to 5% for  
408 coaly facies and values lower than 10% for sandstones, siltstones, and claystones. Calculations  
409 applied to our most porous facies (tight sandstones) led to lean to no TOC contents, consistent with  
410 Rock-Eval measurements. This might indicate that bulk density may not be highly influenced  
411 solely by porosity. In this case, porosity changes between our facies may be considered negligible.  
412 It may also be noted that all rock facies contain the same type of mineralogy (only grain size classes  
413 change) ([Hering et al., 1976](#); [Fleck, 2001](#)), with densities ranging from 2.57 g/cm<sup>3</sup> for sandstones  
414 to 2.7 g/cm<sup>3</sup> for claystone. Well-log density of our coal varies between 1.1 g/cm<sup>3</sup> and 1.8 g/cm<sup>3</sup>.

415 The density contrast between organic matter and sandstones as well as siltstones may thus be  
416 considered as similar. In regards to the above-mentioned considerations, the changes in the bulk  
417 density well-log signal may then be essentially a function of kerogen content. This might explain  
418 why the Schmoker method may be efficient in the calculation of the TOC in the present case study.

419 The presence of pyrite significantly impacts well-log responses, particularly in terms of density  
420 and electrical resistivity, thereby influencing interpretations and calculations based on these  
421 parameters, such as the determination of Total Organic Carbon (TOC) using methods like the  
422 Schmoker or  $\Delta\log R$  techniques. Studies by [Clavier \*et al.\* \(1976\)](#), [Kennedy \(2004\)](#), and [Jiang \*et al.\* \(2018\)](#)  
423 [\(2018\)](#) have extensively documented these effects.

424 Pyrite is distinct from other components of organic-rich rocks due to its very low resistivity and  
425 high density. In claystone layers deposited in marine environments, the presence of pyrite can affect  
426 log signals and, consequently, TOC calculations. To address this, new methods have been  
427 developed to correct for pyrite influence in clay-rich samples. [Jiang \*et al.\* \(2018\)](#) incorporated  
428 pyrite volume considerations into their updated equation based on density to improve accuracy.

429 In this study, 20 sandstone samples, 14 claystone and siltstone samples, 17 shaly coal samples, and  
430 36 coal samples were analyzed using X-ray diffraction (XRD) and petrographic methods. The  
431 pyrite content in these samples is very low, averaging 0.50% in clays and siltstones, 0.8% in  
432 carbonaceous clays, approximately 1% in clayey coals, and nearly 0% in coals ([Fig. 13](#)). This low  
433 pyrite content reflects the fluvial-lacustrine depositional environment, which is isolated from  
434 marine settings and therefore lacks sulfate, resulting in kerogen that is low in pyrite. This suggests  
435 that the Schmoker method is well adapted and needs some adjustment of the coefficients A and B  
436 to provide accurate values for TOC Rock-Eval measurements ([Section 4.1](#)).

437 However, [Section 4.2](#) demonstrates that the  $\Delta\log R$  method results in a tenfold underestimation of  
438 TOC compared to Rock-Eval measurements on our samples. [Kennedy \(2004\)](#) noted that pyrite  
439 effects on electric resistivity tools are significant, as at concentrations above a few per cent, pyrite  
440 can reduce formation electric resistivity. [Sondergeld et al. \(2010\)](#) explain that pyrite in organic-  
441 rich intervals can substantially affect TOC evaluation due to its conductive nature, which reduces  
442 rock resistivity and decreases  $\Delta \log R$ . [Sondergeld et al. \(2010\)](#) applied a correction factor of 4 to  
443 their TOC calculations for marine shales.

444 Within LCB samples analyzed here, the maximum pyrite content reaches 1 % ([Fig. 13](#)), which  
445 might partially affect the underestimation of TOC but does not fully explain the tenfold discrepancy  
446 observed. This suggests that other factors, such as water saturation, may also perturb resistivity  
447 signals, as discussed below.

448 [Passey et al. \(1990\)](#) suggest that the presence of coal intervals induces a significant resistivity  
449 deflection compared to adjacent intervals such as sandstones, siltstones, and shales. Indeed,  
450 [Telford et al. \(1990\)](#) measured high resistivity values ranging from  $0.6 \times 10^5$  to  $1 \times 10^5$  Ohm.m on  
451 dry bituminous coal samples. This may account for  $\Delta\log R$  values in accordance with high TOC of  
452 coaly intervals. However, the resistivity increase observed in the well-logs here is not as strong as  
453 expected.

454 [Figure 14](#) recalls the data presented in [Figure 10](#) with the addition of TOC vs  $\Delta\log R$  data obtained  
455 for sub-bituminous and bituminous coal from the literature. The dark shaded area is relative to dry  
456 coal samples for which  $\Delta\log R$  values are calculated using Equation (3) with sonic slowness of 150  
457  $\mu\text{s}/\text{ft}$  (maximum observed in our well-log data for coal layers), resistivity values for dry coal  
458 ([McCabe and Tholey.,1945](#); [Telford et al., 1990](#)), ([Tab. 3](#)) versus TOC data chosen from literature

459 for pure coals of various rank ([Mastalerz et al., 2011](#)) ([Tab. 3](#)). These values once positioned in  
460 [Figure 14](#) suggest the true relationship that  $\Delta\log R$  and TOC should have for dry coal layers. The  
461 blue shaded area is relative to wet coal samples for which  $\Delta\log R$  values are similarly calculated,  
462 but using resistivity for wet coal from literature ([Tab. 3](#)). These values illustrate the  $\Delta\log R$  and  
463 TOC for wet coal seams. It is noteworthy that these results do align with the TOC vs  $\Delta\log R$   
464 relationship of our wells and sample sets. This implies that the water saturation of our coal-rich  
465 layers significantly influences the calculations. Indeed, the presence of moisture decreases  
466 resistivity ([McCabe and Tholey., 1945](#); [Keskinsezer et al., 2019](#)) and hence the TOC vs  $\Delta\log R$   
467 relationship presents a greater slope than for dry coal. This slope approaches that observed for TOC  
468 values obtained by Rock-Eval measurements, completed by TOC values calculated using the  
469 method by [Schmoker \(1979, 1981\)](#). This suggests that the  $\Delta\log R$  values calculated from our well  
470 log data is strongly underestimated because it is influenced by the presence of formation water in  
471 coal beds. Indeed, in Fols 1A and Dbl S1 wells, resistivity values for coal beds are only 300 to 400  
472 Ohm.m while a dense fracture network is observed ([Privalov et al., 2022](#)).

473 In [figure 14](#), the light gray shaded area represents TOC values calculated for dry (dark shaded area)  
474 and wet coal (blue shaded area) using equation (6) with a LOM of 10.6. In all cases, TOC is strongly  
475 underestimated for TOC > 10% (as observed for [figure 6](#), track 1, 14, and 15). This suggests that the  
476 calibration equation proposed by [Passey et al. \(1990\)](#) for marine shale to determine TOC from  
477 resistivity data may not be valid for coal layers. As suggested earlier, our calibration equations  
478 ([Figs. 11 and 12](#)) may be used for other wells to overcome this problem. However, a more thorough  
479 approach would be to measure laboratory resistivity and sonic slowness of dry and water-saturated  
480 samples for major coaly lithologies and establish the relationship to Rock-Eval TOC to propose a  
481 new  $\Delta\log R$  vs. TOC equation.

482 The observation that moisture decreases resistivity has been demonstrated by [McCabe and Tholey](#)  
483 [\(1945\)](#) and [Keskinsezer et al. \(2019\)](#). In Table 4, resistivity data for dry coal samples were compiled  
484 from references such as [McCabe and Tholey \(1945\)](#) and [Telford et al. \(1990\)](#), covering various  
485 coal ranks. Additional data were sourced from laboratory measurements ([McCabe and](#)  
486 [Tholey.,1945](#)), where samples were saturated with water for 24 hours. These measurements reveal  
487 that resistivity decreases significantly upon water saturation, mirroring the conditions in water-  
488 saturated coal seams. In this study, the analysis was extended by calculating the  $\Delta\log R$  separation  
489 under both dry and wet conditions. The results show that the separation decreases when samples  
490 are wet, comparable to what occurs in situ within water-saturated coal seams. Consequently, TOC  
491 values calculated under wet conditions using the original  $\Delta\log R$  method were significantly  
492 underestimated compared to expected values reported by [Mastalerz et al. \(2011\)](#) for similar coal  
493 ranks. Figure 14 illustrates the relationship between expected TOC values and  $\Delta\log R$   
494 measurements for wet samples. The data points align more closely with results obtained from the  
495 corrected equations proposed in this study. This finding highlights the importance of conducting  
496 sonic and resistivity measurements under varying moisture conditions. To improve TOC estimates,  
497 laboratory testing is recommended to measure  $\Delta\log R$  separation and TOC (via Rock-Eval) for coal  
498 samples of different ranks under wet conditions. Developing new, tailored equations that relate  
499  $\Delta\log R$  separation (between sonic and resistivity logs) to TOC would enhance accuracy, particularly  
500 for values exceeding 10 wt%, and provide a more reliable model derived from laboratory data.

501 [Kenomore et al. \(2017\)](#) explained that in shale reservoirs, when the formation's porosity is less than  
502 3–4%, resistivity increases significantly due to the absence of electrically conductive fluids.  
503 Consequently, the  $\Delta\log R$  separation can be very high and should not be used under such conditions.  
504 In this case study, the matrix porosity appears to be less than 4%, which places the coal layers

505 within this category where resistivity is expected to increase. However, in coalbed methane (CBM)  
506 reservoirs, the effective porosity is predominantly defined by the fracture porosity within the cleat  
507 system. This cleat porosity can significantly counteract the impact of low matrix porosity, as the  
508 fractures are often filled with water, which dramatically reduces resistivity. This phenomenon  
509 underscores a key aspect of the unconventional nature of these CBM reservoirs-Source Rock,  
510 [Tables 4](#) and [5](#) present the determination coefficient and the Root Mean Squared Error (RMSE)  
511 calculated for each of the proposed TOC calculation equations using well log data of Fols 1A and  
512 Dbl S1 wells. [Figures 6](#) and [7](#) present in yellow the difference between TOC calculated using the  
513 different equations proposed and values obtained by using the equation based on [Schmoker \(1979,](#)  
514 [1981\)](#). RMSE allows to rank of the proposed equations to calculate TOC as follows: i) modified  
515  $\Delta\log R$  (Eqs. [11](#) and [12](#)) ii) multivariate analysis (Eqs. [19](#) and [20](#)) iii) TOC  $\Delta\log R$  equation  
516 calibrated with Rock-Eval and calculated TOC using the method by [Schmoker \(1979, 1981\)](#). (Eqs.  
517 [13](#) and [18](#)).

## 518 **6. Conclusion**

519 In the literature, TOC determination using well-logs is most commonly applied to quite  
520 homogenous marine shale deposits. Our objective was to adapt such techniques to the very  
521 heterogeneous fluvial deposits in two reference wells of the Carboniferous Lorraine basin. We  
522 therefore focused on Schmoker's method (1978, 1979),  $\Delta\log R$  (Passey et al. 1990) and multivariate  
523 regression analysis in accordance to the well-log data available. Continuous TOC determination  
524 profiles were obtained despite the complexity of facies changes. The average TOC content in the  
525 shales of Fols 1A Well ranges from 3.5 wt % to 4.5 wt %, while for coal layers, it ranges from 40  
526 wt % to 50 wt %. In Dbl S1 Well, the average TOC content in shales varies from 4.8 wt % to 6.2

527 wt %, while in coal layers, it ranges from 30 wt % to 45 wt %. Accordingly, quality assessment  
528 based on TOC (Kenomore et al., 2017), source rocks range from very good for shaly lithologies to  
529 excellent for coal layers.

530 The Schmoker method lead to best results but can only be used when density logs are available. In  
531 the case only resistivity and sonic data are accessible, a proposed modified  $\Delta\log R$  equations was  
532 utilized as the original  $\Delta\log R$  method tends to significantly underestimate values for coaly  
533 lithologies. Alternatively, if gamma ray, sonic, and resistivity data are present, the use of the  
534 derived equations from the multivariate regression analysis is recommended. This combination of  
535 available well-log data in this basin, along with additional Rock-Eval and petrophysical data from  
536 core samples, can serve as the basis for future studies employing machine learning applications  
537 that reduce error and increase the precision of TOC predictions in the Lorraine Basin and could be  
538 further tested on other coal-rich basins.

539 **Acknowledgments:** The authors would like to thank Prof. Khalid Essa for scientific discussions,  
540 Dr. Alizerrouki ahmed for helping in improve the manuscript, Schlumberger (SLB) for providing  
541 the Techlog© academic license. We are grateful to the editor and the reviewers for their time and  
542 suggestions for improving the manuscript. This research was funded through REssources GAZières  
543 de LORaine (REGALOR) - Research program cofounded Etat (Pacte Lorraine), Région (Région  
544 Grand Est), and Europe (Fond Européen de DEveloppement Régional - FEDER); 2018-2023.

## 545 **References**

546 Alizadeh B, Najjari S, Kadkhodaie-Ilkhchi, A. 2012. Artificial neural network modeling and  
547 cluster analysis for organic facies and burial history estimation using well log data : A case  
548 study of the South Pars Gas Field, Persian Gulf, Iran. *Computers & Geosciences* 45: 261-269.

- 549 Allouti, S., 2024. Nature, distribution et potentiel gazier des charbons et roches-mères du bassin  
550 carbonifère de Lorraine: contribution à l'estimation des ressources en gaz. Ph.D thesis,  
551 Lorraine University, 341pp.
- 552 Alpern B, Choffe M, Lachkar G, Liabeuf JJ. 1969. Synthèse des zonations palynologiques des  
553 bassins houillers de Lorraine et de Sarre. *Revue de Micropaléontologie* 11(4): 217-221.
- 554 Amiri Bakhtiar H, Telmadarreie A, Shayesteh M, Heidari Fard MH, Talebi H, Shirband Z. 2011.  
555 Estimating Total Organic Carbon Content and Source Rock Evaluation, Applying  $\Delta\log R$  and  
556 Neural Network Methods : Ahwaz and Marun Oilfields, SW of Iran. *Petroleum Science and  
557 Technology* 29(16) : 1691-1704.
- 558 Barrabé L, Feys R. 1965. Géologie du charbon et des bassins houillers. Paris: Masson et Cie ed.  
559 230 p.
- 560 Bessereau G, Carpentier B, Huc AY. 1991. Wireline Logging And Source Rocks-Estimation Of  
561 Organic Carbon Content By The Carbolbg@ Method. *The Log Analyst* 32(03).
- 562 Bolandi V, Kadkhodaie A, Farzi R. 2017. Analyzing organic richness of source rocks from well  
563 log data by using SVM and ANN classifiers : A case study from the Kazhdumi formation,  
564 the Persian Gulf basin, offshore Iran. *Journal of Petroleum Science and Engineering* 151:  
565 224-234.
- 566 Chan, SA, Hassan AM, Usman M, Humphrey JD, Alzayer Y, Duque, F. 2022. Total organic  
567 carbon (TOC) quantification using artificial neural networks : Improved prediction by  
568 leveraging XRF data. *Journal of Petroleum Science and Engineering* 208: 109302.
- 569 Chatterjee R, Paul, S. 2013. Classification of coal seams for coal bed methane exploitation in  
570 central part of Jharia coalfield, India–A statistical approach. *Fuel* 111: 20-29.
- 571 Clavier C, Heim A, Scala C. 1976. Effect of pyrite on resistivity and other logging measurements.  
572 In: SPWLA Annual Logging Symposium, SPWLA-1976.
- 573 Cranganu C, Dimitrijevic D. 2016. Intelligent Modeling Approaches in Petroleum Geosciences.  
574 In: Determining the Total Organic Carbon (TOC) in Marcellus Shale, NY State -  
575 International Conference of Gas, Oil and Petroleum Engineering, Las Vegas, (November 14  
576 - 16, 2016).
- 577 Diessel CFK. 1992. "Coal facies and depositional environment." Coal depositional systems.  
578 Springer Ed., 721 p.
- 579 Donsimoni M. 1981. Le bassin houiller lorrain. Mémoire. *Bureau des recherches géologiques et  
580 minières*. Orléans. 117, 99 p.

- 581 Elkatatny S. 2019. A Self-Adaptive Artificial Neural Network Technique to Predict Total Organic  
582 Carbon (TOC) Based on Well Logs. *Arabian Journal for Science and Engineering* 44(6):  
583 6127-6137.
- 584 Espitalié J, Deroo G, Marquis F. 1985. La pyrolyse Rock-Eval et ses applications. *Rev. Inst. franç.*  
585 *Pétrole, Technip, Paris* 40(5): 563-579.
- 586 Fleck S. 2001. Corrélation entre géochimie organique, sédimentologie et stratigraphie séquentielle  
587 pour la caractérisation des paléoenvironnements de dépôt. Thèse, *université Henri Poincaré,*  
588 *Nancy 1* : 387 p.
- 589 Fleck S, Michels R, Izart A, Elie, Landais P. 2001. Palaeoenvironmental assessment of  
590 Westphalian fluvio-lacustrine deposits of Lorraine (France) using a combination of organic  
591 geochemistry and sedimentology. *International Journal of Coal Geology* 48(1-2): 65-88.
- 592 Ghosh S, Chatterjee R, Shanker P. 2016. Estimation of ash, moisture content and detection of coal  
593 lithofacies from well logs using regression and artificial neural network modelling. *Fuel* 177:  
594 279-287.
- 595 Gradstein FM, Ogg JG, Schmitz MD, Ogg GM. 2020. Geologic time scale 2020, 2<sup>nd</sup> ed. Elsevier.  
596 1357p.
- 597 Gunzburger Y. 2019. Le gaz de charbon en Lorraine : Quelle intégration dans le territoire? CNRS  
598 Éditions via OpenEdition. 130 p.
- 599 Hemelsdaël R., Averbuch O., Beccaletto L., Izart A., Marc S., Capar L., Michels R. 2023. A  
600 deformed wedge-top basin inverted during the collapse of the Variscan belt: the Permo-  
601 Carboniferous Lorraine basin (NE France). *Tectonics*, 42, e2022TC007668.
- 602 Henk A. 1993. Late orogenic basin evolution in the Variscan Internides : The Saar-Nahe Basin,  
603 southwest Germany. *Tectonophysics* 223(3-4): 273-290.
- 604 Hering O. 1976. Petrographische Beschreibung und Deutung der erbohrten Schichten (Saar 1).  
605 *Geologisches Jahrbuch* 27: 91.
- 606 Hollub VA, Schafer, PS. 1992. A guide to coalbed methane operations. Chicago (USA): Gas  
607 Research Institute.
- 608 Hood A, Gutjahr, CCM, Heacock R L. 1975. Organic metamorphism and the generation of  
609 petroleum. *AAPG bulletin*, 59(6): 986-996.
- 610 Hu H, Su R, Liu C, Meng L. 2016. The method and application of using Generalized DlogR  
611 technology to predict the organic carbon content of continental deep source rocks. *Natural.*  
612 *Gas. Geosci* 27 (1): 149-155.

- 613 Huang Z, Williamson MA. 1996. Artificial neural network modelling as an aid to source rock  
614 characterization. *Marine and Petroleum Geology* 13(2): 277-290.
- 615 Izart A, Palain C, Malartre F, Fleck S, Michels R. 2005. Paleoenvironments, paleoclimates and  
616 sequences of Westphalian deposits of Lorraine coal basin (Upper Carboniferous, NE France).  
617 *Bulletin de la Société géologique de France*, 176(3): 301-315.
- 618 Izart A, Barbarand J, Michels R, Privalov VA. 2016. Modelling of the thermal history of the  
619 Carboniferous Lorraine Coal Basin: Consequences for coal bed methane. *International*  
620 *Journal of Coal Geology* 168: 253-274.
- 621 Izart, A., Opluštil, S., Michels, R., Voigt, S., Barbarand, J., Blaise, T., Laurin, J., Schmitz, M.,  
622 Hartkopf, C., Allouti, S., Hemelsdaël, R. 2025. New high precision U-Pb zircon ages of the  
623 Saar-Lorraine (SW Germany-NE France) Basin. *International Journal of Coal Geology*, 302,  
624 104724. <https://doi.org/10.1016/j.coal.2025.104724>.
- 625 Jiang S, Mokhtari M, Borrok D, Lee J. 2018. Improving the total organic carbon estimation of the  
626 Eagle Ford shale with density logs by considering the effect of pyrite. *Minerals* 8(4): 154.
- 627 Kamali MR, Mirshady AA. 2004. Total organic carbon content determined from well logs using  
628  $\Delta\text{LogR}$  and Neuro Fuzzy techniques. *Journal of petroleum Science and Engineering* 45(3-4):  
629 141-148.
- 630 Karacan CÖ. 2009. Reservoir rock properties of coal measure strata of the Lower Monongahela  
631 Group, Greene County (Southwestern Pennsylvania), from methane control and production  
632 perspectives. *International Journal of Coal Geology*, 78(1): 47-64.
- 633 Kennedy MC. 2004. Gold Fool's: Detecting, quantifying and accounting for the effects of Pyrite  
634 on modern logs. In: *SPWLA Annual Logging Symposium*. SPWLA-2004.
- 635 Kenomore M, Hassan M, Dhakal H, Shah A. 2017. Total organic carbon evaluation of the  
636 Bowland Shale Formation in the Upper Bowland of the Widmerpool Gulf. *Journal of*  
637 *Petroleum Science and Engineering* 150: 137-145.
- 638 Keskinsezer A. 2019. Determination of coal layers using geophysical well-logging methods for  
639 correlation of the Gelik-Zonguldak and Kazpınar-Amasra (Bartın) coalfields, Turkey.  
640 *Geomechanics and Geophysics for Geo-Energy and Geo-Resources* 5(3): 223-235.
- 641 Khoshnoodkia M, Mohseni H, Rahmani O, Mohammadi A. 2011. TOC determination of Gadvan  
642 Formation in South Pars Gas field, using artificial intelligent systems and geochemical data.  
643 *Journal of Petroleum Science and Engineering* 78(1): 119-130.

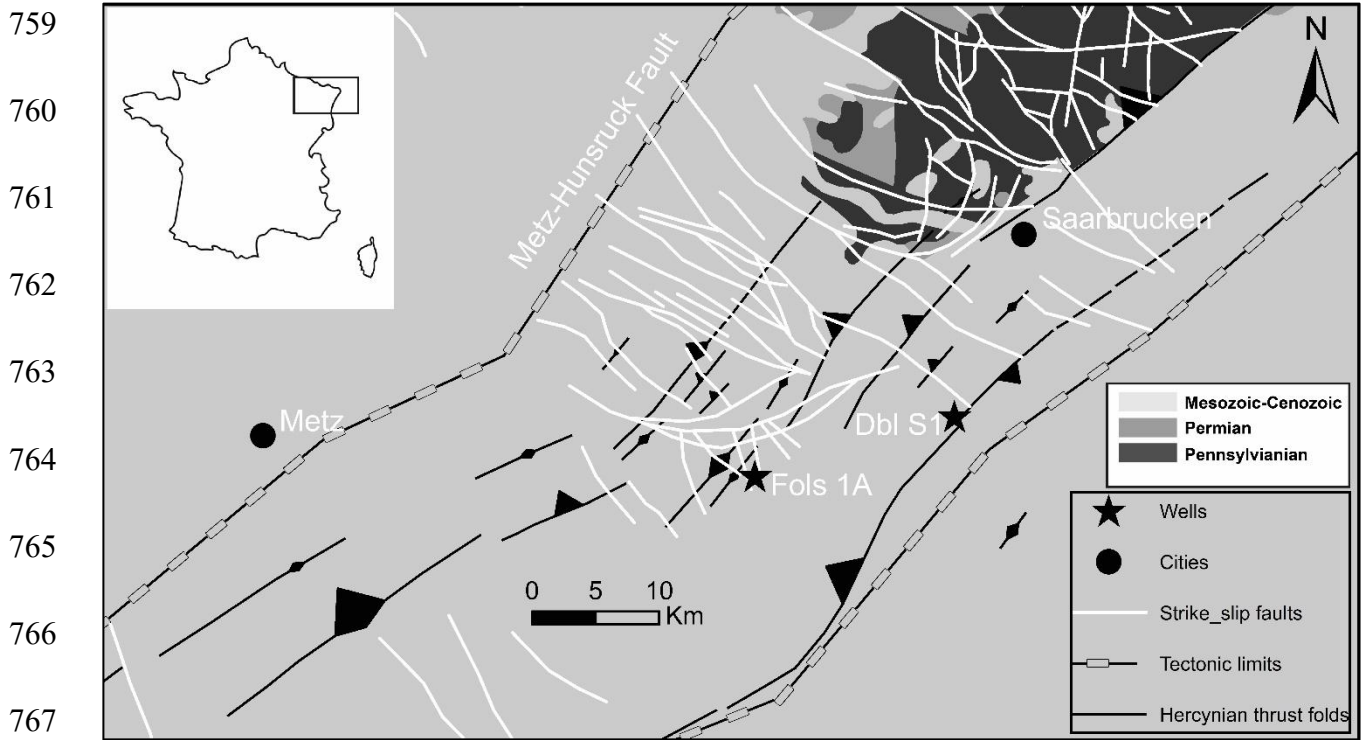
- 644 Laveine JP. 1974. Précisions sur la répartition stratigraphique des principales espèces végétales  
645 du Carbonifère supérieur de Lorraine. *CR Acad. Sci. Paris* 278(D): 851-854.
- 646 Li M, Zhang C. 2023. An Improved Method to Accurately Estimate TOC of Shale Reservoirs and  
647 Coal-Measures. *Energies* 16(6): 2905.
- 648 Liu H, Mou J, Cheng Y. 2015. Impact of pore structure on gas adsorption and diffusion dynamics  
649 for long-flame coal. *Journal of Natural Gas Science and Engineering* 22: 203-213.
- 650 Mahmoud AAA, Elkatatny S, Mahmoud M, Abouelresh M, Abdulraheem A, Ali A, 2017.  
651 Determination of the total organic carbon (TOC) based on conventional well logs using  
652 artificial neural network. *International Journal of Coal Geology* 179: 72-80.
- 653 Mahmoud AA, Elkatatny S, Ali AZ, Abouelresh, M, Abdulraheem A. 2019. Evaluation of the  
654 total organic carbon (TOC) using different artificial intelligence techniques. *Sustainability*  
655 11(20): 5643.
- 656 Mann, U., & Müller, P. J. (1988). Source rock evaluation by well log analysis (Lower Toarcian,  
657 Hils syncline). In *Organic Geochemistry In Petroleum Exploration* (p. 109-119). Elsevier.
- 658 Mann U, Leythaeuser D, Müller PJ. 1986. Relation between source rock properties and wireline  
659 log parameters : An example from Lower Jurassic Posidonia Shale, NW-Germany. *Organic*  
660 *geochemistry* 10(4-6): 1105-1112.
- 661 Mastalerz M, Drobniak A, Hower J, O’Keefe J. 2011. Spontaneous Combustion and Coal  
662 Petrology. In: Stracher GB, Prakash A, Sokol EV, ed. *Coal and peat fires: a global*  
663 *perspective: coal-geology and combustion*. Elsevier. pp. 48-62.
- 664 Mavor M, Close JC, McBane RA. 1994. Formation evaluation of exploration coalbed-methane  
665 wells. *SPE Formation Evaluation* 9(04): 285-294.
- 666 McCabe LC, Tholey CC. 1945. Physical Properties of Coals. In: Schmidt LD, Lowry HH, ed.  
667 *Chemistry of coal utilization*. New York: Wiley. pp. 310-336
- 668 McCabe PJ. 1985. Depositional Environments of Coal and Coal-Bearing Strata. In: Rahmani RA,  
669 Flores RM, ed. *Sedimentology of Coal and Coal-Bearing Sequences*. New York: Wiley. Pp  
670 11-42.
- 671 Meissner FF. 1978. Petroleum geology of the Bakken formation Williston basin, North Dakota  
672 and Montana. In: *Proceedings of 1978 Williston Basin Symposium*, Montana Geological  
673 Society, Billings. pp. 207-227.
- 674 Mendelzon JD, Toksoz, MN.1985. Source rock characterization using multivariate analysis of log  
675 data. In: *SPWLA Annual Logging Symposium*, SPWLA-1985. pp. 253-330

- 676 Meng S-P, Liu C-L, Ji Y-M. 2013. Geological conditions of coalbed methane and shale gas  
677 exploitation and their comparison analysis. *Journal of China Coal Society* 38(5): 728-736.
- 678 Meyer BL, Nederlof MH. 1984. Identification of source rocks on wireline logs by  
679 density/resistivity and sonic transit time/resistivity crossplots. *AAPG bulletin* 68(2): 121-129.
- 680 Morin RH. 2005. Hydrologic properties of coal beds in the Powder River Basin, Montana I.  
681 Geophysical log analysis. *Journal of Hydrology*, 308(1-4): 227-241.
- 682 Nezhad YA, Moradzadeh A, Kamali MR. 2018. A new approach to evaluate Organic  
683 Geochemistry Parameters by geostatistical methods : A case study from western Australia.  
684 *Journal of Petroleum Science and Engineering* 169: 813-824.
- 685 Nixon RP. 1973. Oil source beds in Cretaceous Mowry Shale of northwestern interior United  
686 States. *AAPG bulletin*, 57(1): 136-161.
- 687 Nyakilla EE, Silingi SN, Shen C, Jun G, Mulashani AK, Chibura PE. 2022. Evaluation of Source  
688 Rock Potentiality and Prediction of Total Organic Carbon Using Well Log Data and  
689 Integrated Methods of Multivariate Analysis, Machine Learning, and Geochemical Analysis.  
690 *Natural Resources Research* 31(1): 619-641.
- 691 Passey QR, Creaney S, Kulla JB, Moretti FJ, Stroud JD. 1990. A practical model for organic  
692 richness from porosity and resistivity logs. *AAPG bulletin* 74(12): 1777-1794.
- 693 Privalov V, Pironon J, de Donato P, Michels R, Izart A, Morlot C, Panova O. 2022. Multi-scale  
694 structural inheritance of fracture systems pattern in coal-bearing measures of the Lorraine-  
695 Saar coal Basin. *Geofizičeskij žurnal*, 44(1): 40-54.
- 696 Pruvost P. 1934. Bassin houiller de la Sarre et de la Lorraine. Description géologique (Etudes des  
697 gîtes minéraux de la France). *Imprimerie Danel, Lille*. 173 p.
- 698 Rider M, Kennedy M. 2011. Sonic or acoustic logs. In: Rider M, Kennedy M, ed. The geological  
699 interpretation of well logs, third ed. Glasgow: Rider-French Consulting Limited. pp. 187-  
700 209.
- 701 Schäfer A. 1989. Variscan molasse in the Saar-Nahe Basin (W-Germany), Upper Carboniferous  
702 and Lower Permian. *Geologische Rundschau* 78(2): 499-524.
- 703 Schäfer A. 2011. Tectonics and sedimentation in the continental strike-slip Saar-Nahe basin  
704 (Carboniferous-Permian, West Germany). *Zeitschrift der Deutschen Gesellschaft für*  
705 *Geowissenschaften* 162(2): 127.
- 706 Schmoker JW. 1979. Determination of organic content of Appalachian Devonian shales from  
707 formation-density logs : Geologic notes. *AAPG Bulletin* 63(9): 1504-1509.

- 708 Schmoker, JW. 1981. Determination of organic-matter content of Appalachian Devonian shales  
709 from gamma-ray logs. *AAPG Bulletin* 65(7): 1285-1298.
- 710 Schmoker JW, Hester TC. 1983. Organic carbon in Bakken formation, United States portion of  
711 Williston basin. *AAPG bulletin* 67(12): 2165-2174.
- 712 Schwarzkopf TA. 1992. Source rock potential (TOC+ hydrogen index) evaluation by integrating  
713 well log and geochemical data. *Organic geochemistry* 19(4-6): 545-555.
- 714 Seidle J. 2011. Geologic Aspects of Coal Gas Reservoir Engineering, in: Seidle J, ed.  
715 Fundamentals of Coalbed Methane Reservoir Engineering. Oklahoma: PennWell  
716 Corporation. pp. 59-88.
- 717 Sondergeld CH, Newsham KE, Comisky JT, Rice MC, Rai CS. 2010. Petrophysical  
718 considerations. In: Proceedings of evaluating and producing shale gas resources. SPE  
719 Unconventional Resources Conference/Gas Technology Symposium. SPE-131768.
- 720 Su X, Wang Q, Lin H, Song J, Guo H. 2018. A combined stimulation technology for coalbed  
721 methane wells : Part 1. Theory and technology. *Fuel* 233: 592-603.
- 722 Sun SZ, Sun Y, Sun C, Liu Z, Dong N. 2013. Methods of calculating total organic carbon from  
723 well logs and its application on rock's properties analysis. In: Proceedings of the Geo  
724 Convention. Calgary (Canada). pp. 1-7
- 725 Sutton T. 2014. Wireline Logs for Coalbed Evaluation. In: Thakur P, Schatzel SJ, Aminian K, Ed.  
726 Coal bed methane: From prospect to pipeline. Elsevier, 2014, 93-101
- 727 Telford WM, Geldart LP, Sheriff RE. 1990. Applied geophysics. Cambridge: Cambridge  
728 university press.760 p.
- 729 Termier P.1923. Contribution à la connaissance des» Tonstein «du houiller de la Sarre. *Bull. Soc.*  
730 *géol. France* 4(23): 45-50.
- 731 Thomas L. 2002. Coal geology, 2<sup>nd</sup> ed. A John Wiley & Sons, Ltd. West Sussex. 456p.
- 732 Van Krevelen DW. 1993. Coal : Typology-physics-chemistry-constitution (Coal Science and  
733 Technology). New York: Elsevier. pp. 100.
- 734 Wang P, Peng S, He T. 2018. A novel approach to total organic carbon content prediction in shale  
735 gas reservoirs with well logs data, Tonghua Basin, China. *Journal of Natural Gas Science*  
736 *and Engineering* 55: 1-15.

- 737 Wang P, Peng S, Du W, Feng F. 2017. Prediction model of total organic carbon content on  
738 hydrocarbon source rocks in coal measures based on geophysical well logging. *J. China Coal*  
739 *Soc* 42 (5): 1266-1276.
- 740 Wang Q. 2022. Timeliness Analysis of Coalbed Methane Workover for Reducing Damage to Coal  
741 Reservoirs. *ACS Omega* 7(8): 6956-6962.
- 742 Wood DA. 2023. Predicting total organic carbon from few well logs aided by well-log attributes.  
743 *Petroleum* 9(2): 166-182.
- 744 Yu H, Rezaee R, Wang Z, Han T, Zhang Y, Arif M, Johnson, L. 2017. A new method for TOC  
745 estimation in tight shale gas reservoirs. *International Journal of Coal Geology* 179: 269-277.
- 746 Zhang B, Xu J. 2016. Methods for the evaluation of water saturation considering TOC in shale  
747 reservoirs. *Journal of Natural Gas Science and Engineering* 36: 800-810.
- 748 Zhao B. 2019. Predicting total organic carbon content in marine shale reservoirs with nuclear  
749 logging data. *Xinjing Pet. Geol* 40 (4): 499-504.
- 750 Zhou B, Esterle J. 2008. Toward improved coal density estimation from geophysical logs.  
751 *Exploration Geophysics* 39(2): 124-132.
- 752 Zhu L, Zhang C, Zhang C, Zhou X, Wang J, Wang, X. 2018. Application of Multiboost-KELM  
753 algorithm to alleviate the collinearity of log curves for evaluating the abundance of organic  
754 matter in marine mud shale reservoirs: A case study in Sichuan Basin, China. *Acta*  
755 *Geophysica* 66(5): 983-1000.
- 756 Zhu L, Zhou X, Liu W, Kong Z. 2023. Total organic carbon content logging prediction based on  
757 machine learning : A brief review. *Energy Geoscience* 4(2): 100098.





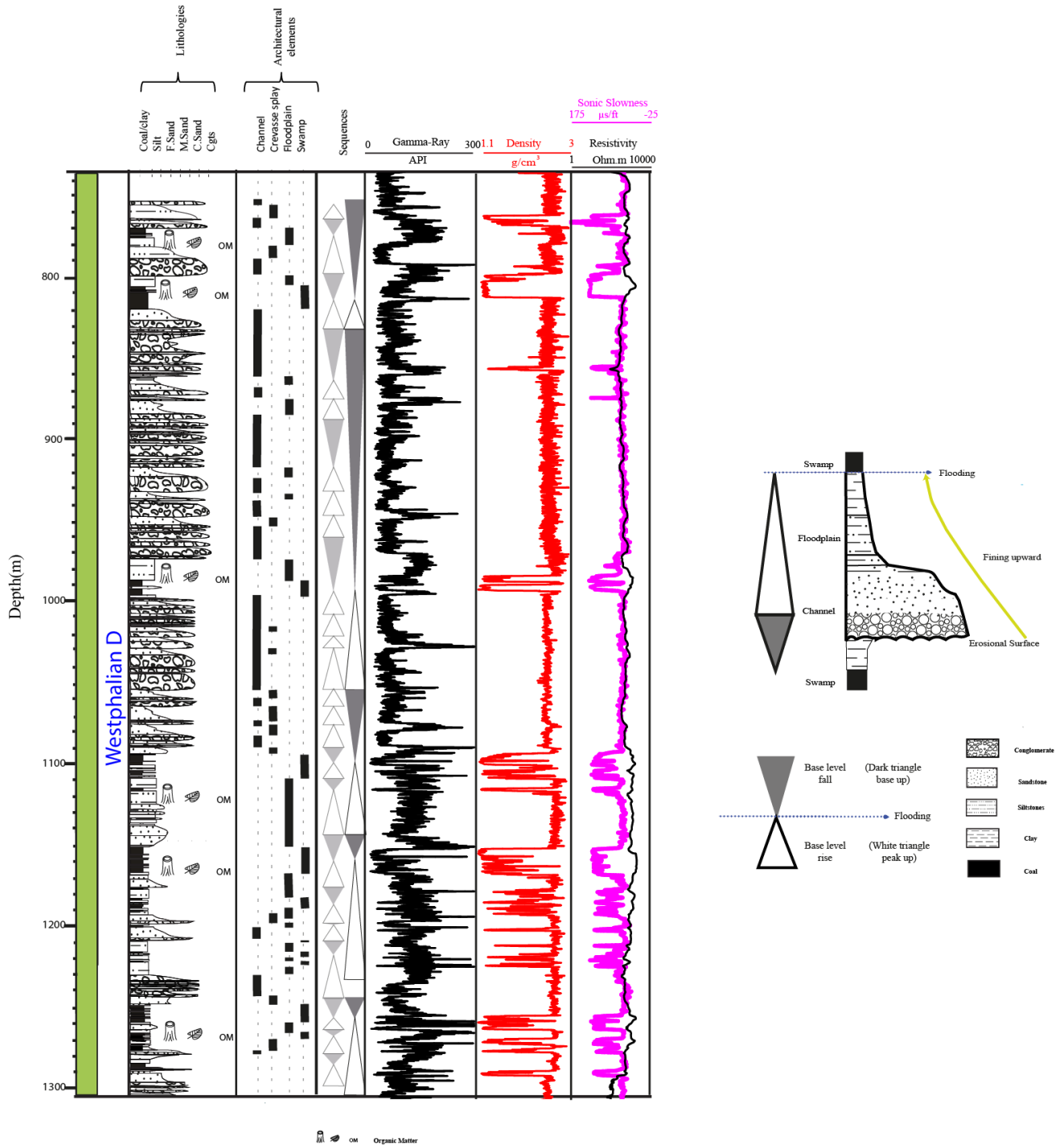
768 **Fig. 1:** Simplified geological map of the Saar-Lorraine Basin showing the location of Folschviller  
769 (Fols 1A) and Diebling (Dbl S1) boreholes. The Carboniferous Basin is accessed by both boreholes  
770 at depths of 700 and 600 meters, respectively. Permian and Carboniferous outcrop in Germany.  
771 Modified after [Pruvost \(1934\)](#), [Donsimoni \(1981\)](#), [Schäfer \(2011\)](#) and [Izart et al. \(2016\)](#).

772

773

774

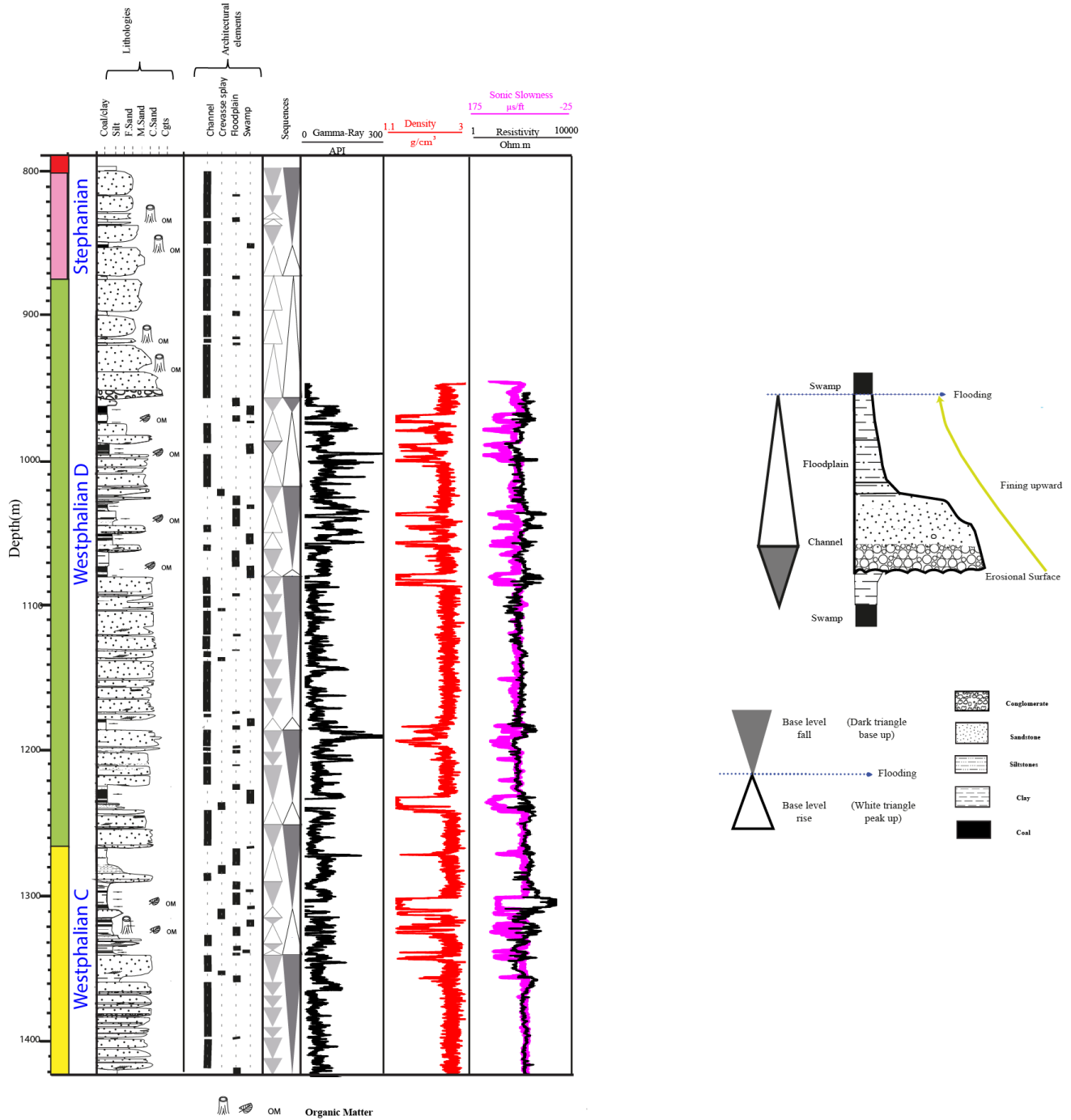
# Fols 1A



775

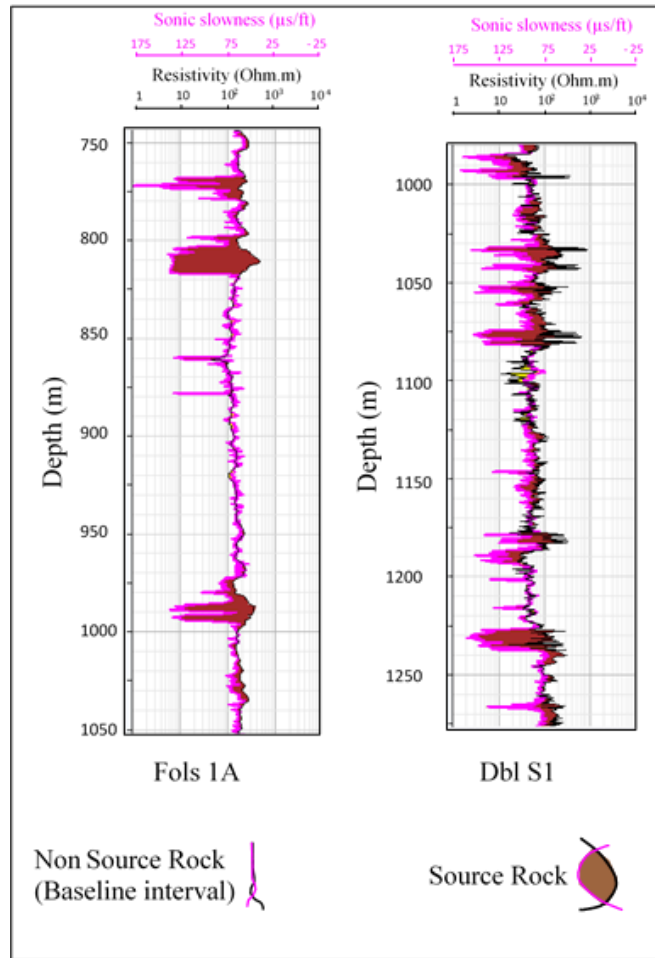
776 **Fig. 2:** Sedimentary logs of Folschviller (Fols 1A) well presenting lithological succession,  
 777 corresponding depositional environments, architectural element log and sedimentary sequences  
 778 representative of the Lorraine Carboniferous basin. Data based on well-logs and core analysis.

Dbl S1



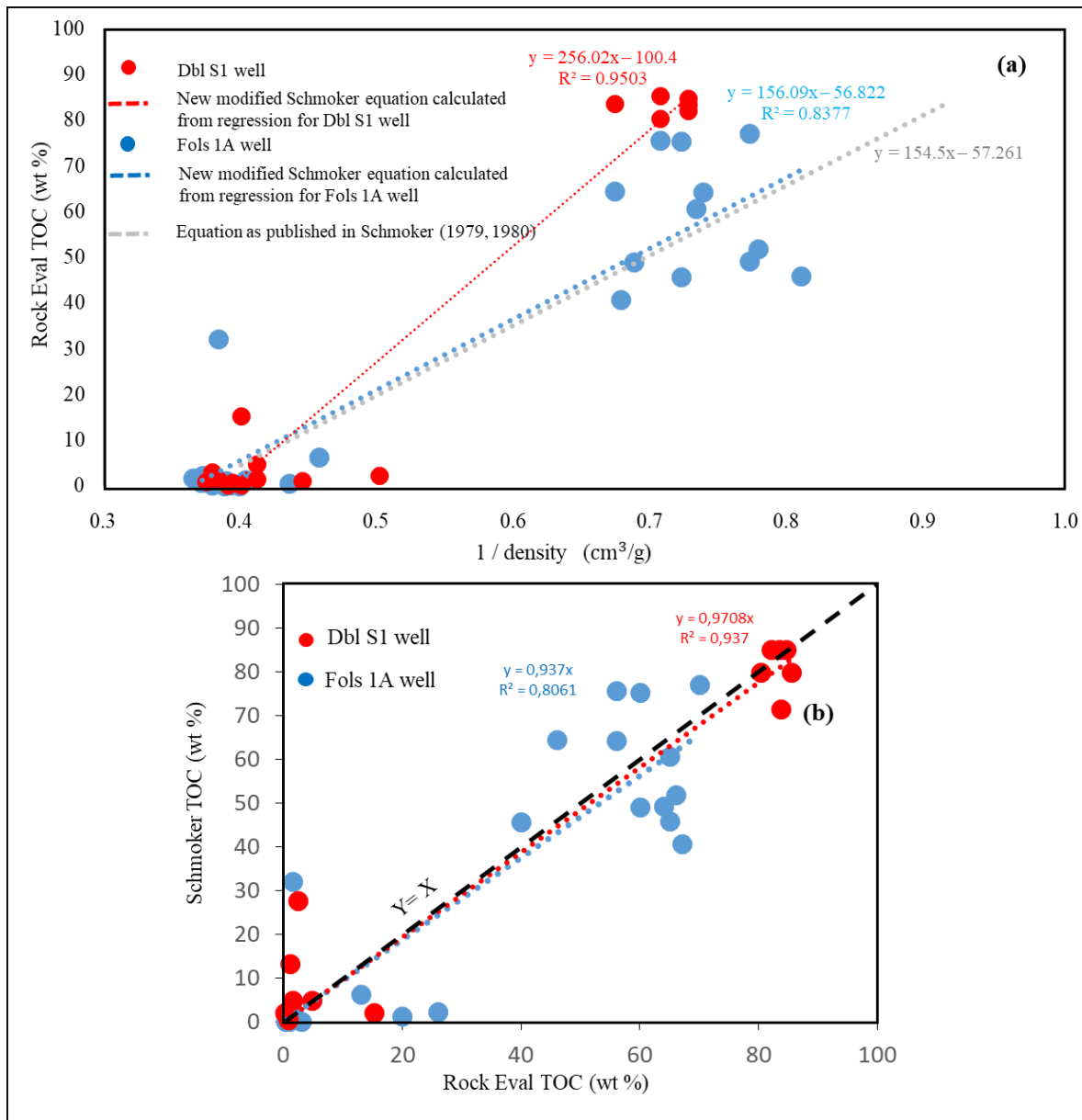
779

780 **Fig. 3:** Sedimentary logs of Diebling (Dbl S1) well presenting lithological succession,  
 781 corresponding depositional environments, architectural element log and sedimentary sequences  
 782 representative of the Lorraine Carboniferous basin. Data based on well-logs and core analysis.



783

784 **Fig. 4:** Sonic/Resistivity Overlay is showing  $\Delta \log R$  separation in the coal rich intervals for Fols 1A  
 785 and Dbls1 wells. The relative scaling and resistivity curves correspond to a 50  $\mu\text{s}/\text{ft}$  increment,  
 786 representing one decade of resistivity.



787

788 **Fig. 5:** Calibration of TOC by [Schmoker \(1979, 1981\)](#): (a) Linear relationship among Rock Eval

789 TOC (wt%) and 1/density (cc/g) in Fols 1A and Dbl S1 wells as calibrated by the method published

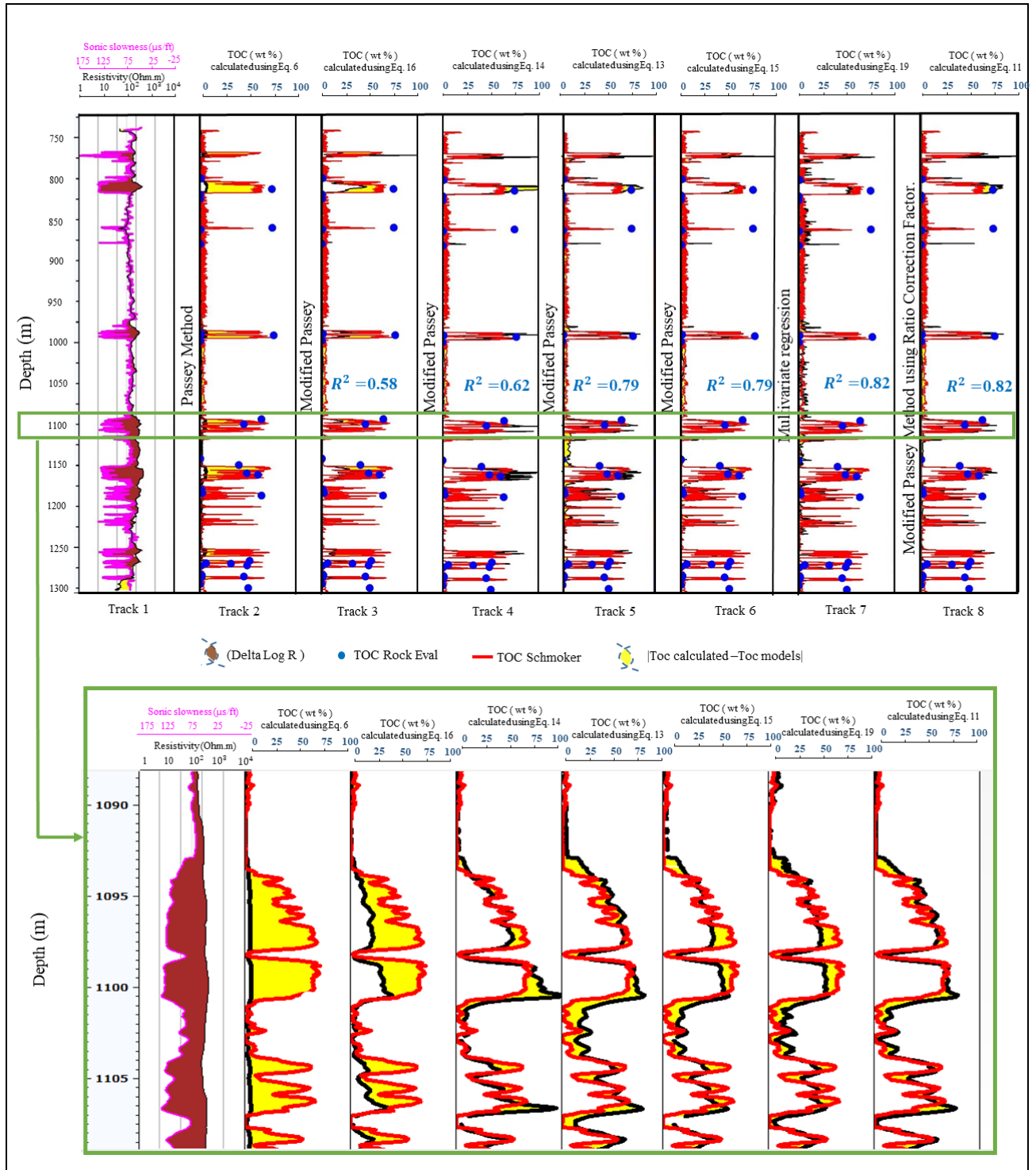
790 by [Schmoker \(1979,1981\)](#); (b) Comparison of Rock Eval TOC with TOC calculated using the

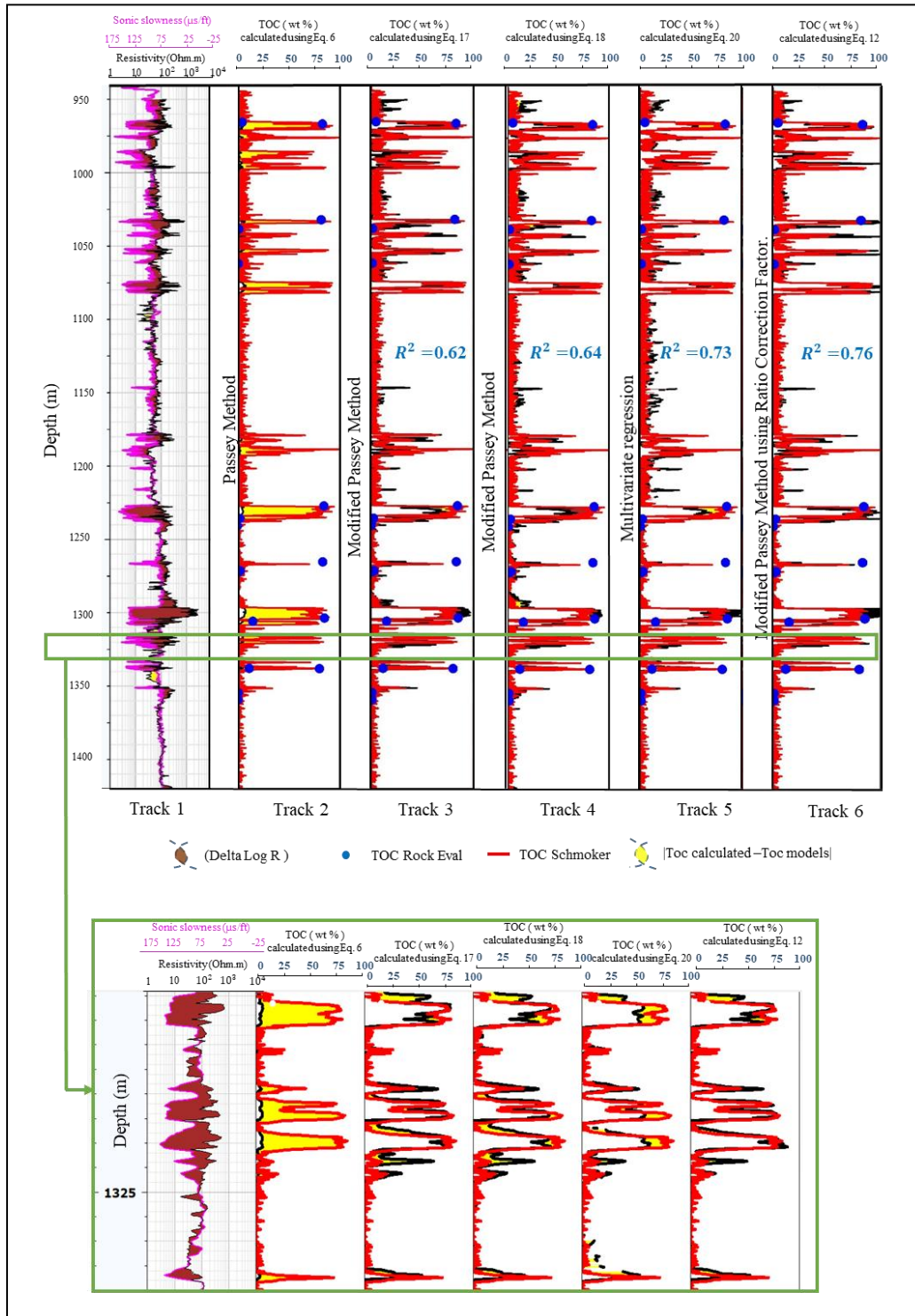
791 equation published by Schmoker for Fols 1A and proposed modified equation for calibration of

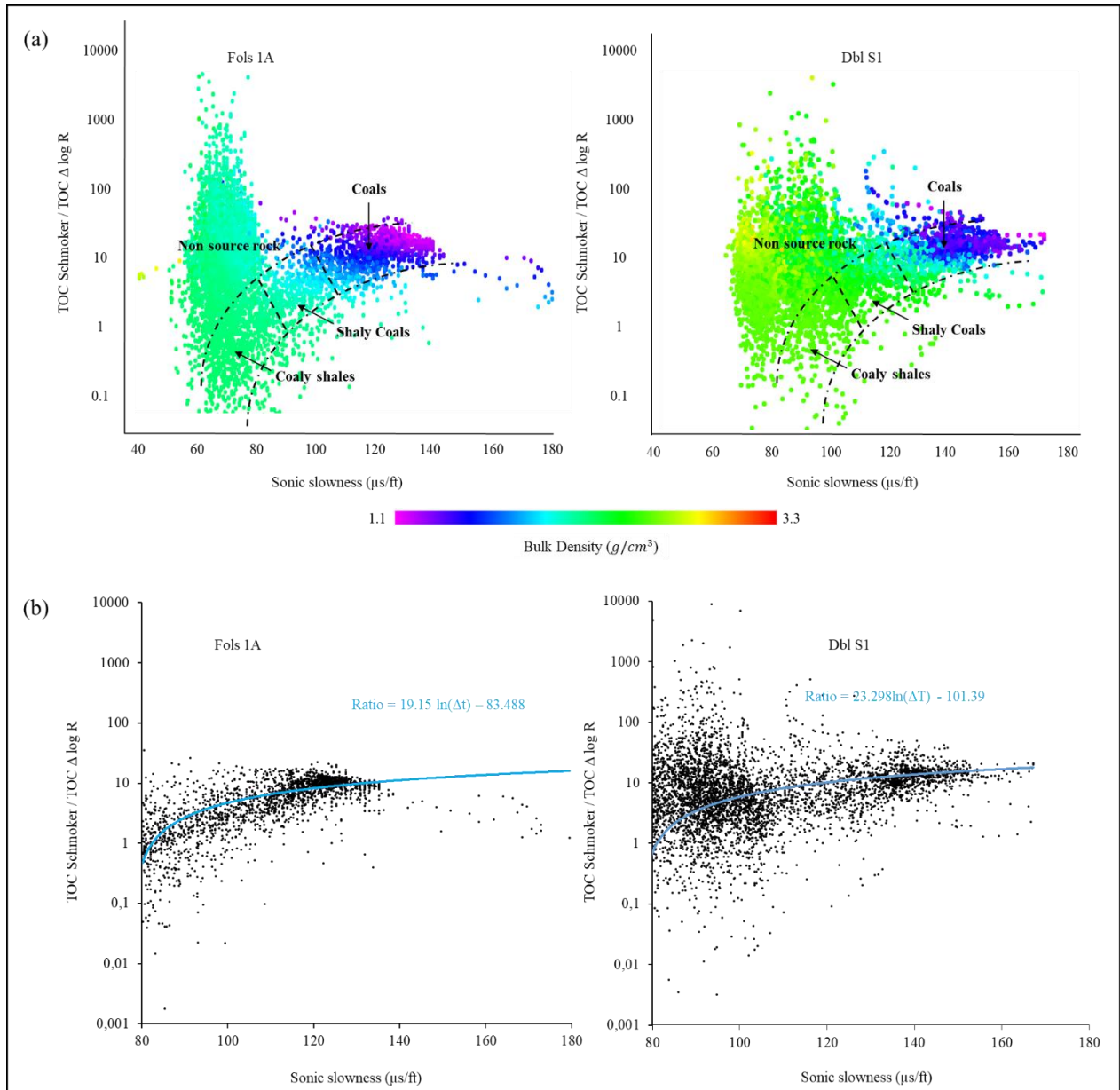
792 Dbl S1 wells.

793

794





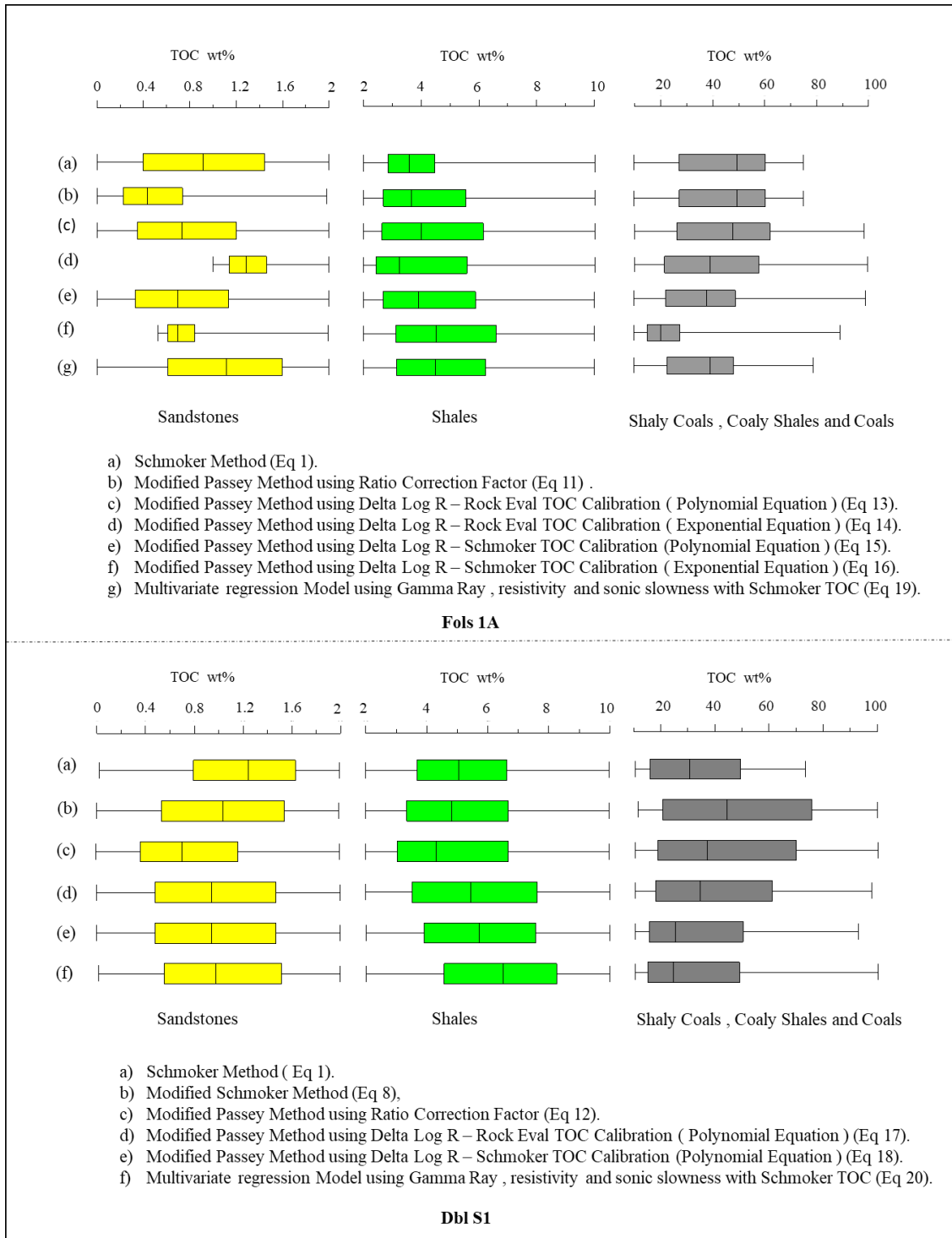


802

803 **Fig. 8:** Calculated TOC ratio using Schmoker and Delta log R methods in Fols 1A and Dbl S1

804 wells: (a) as a function of Sonic Slowness and bulk density: in color code for all lithologies, (b) as

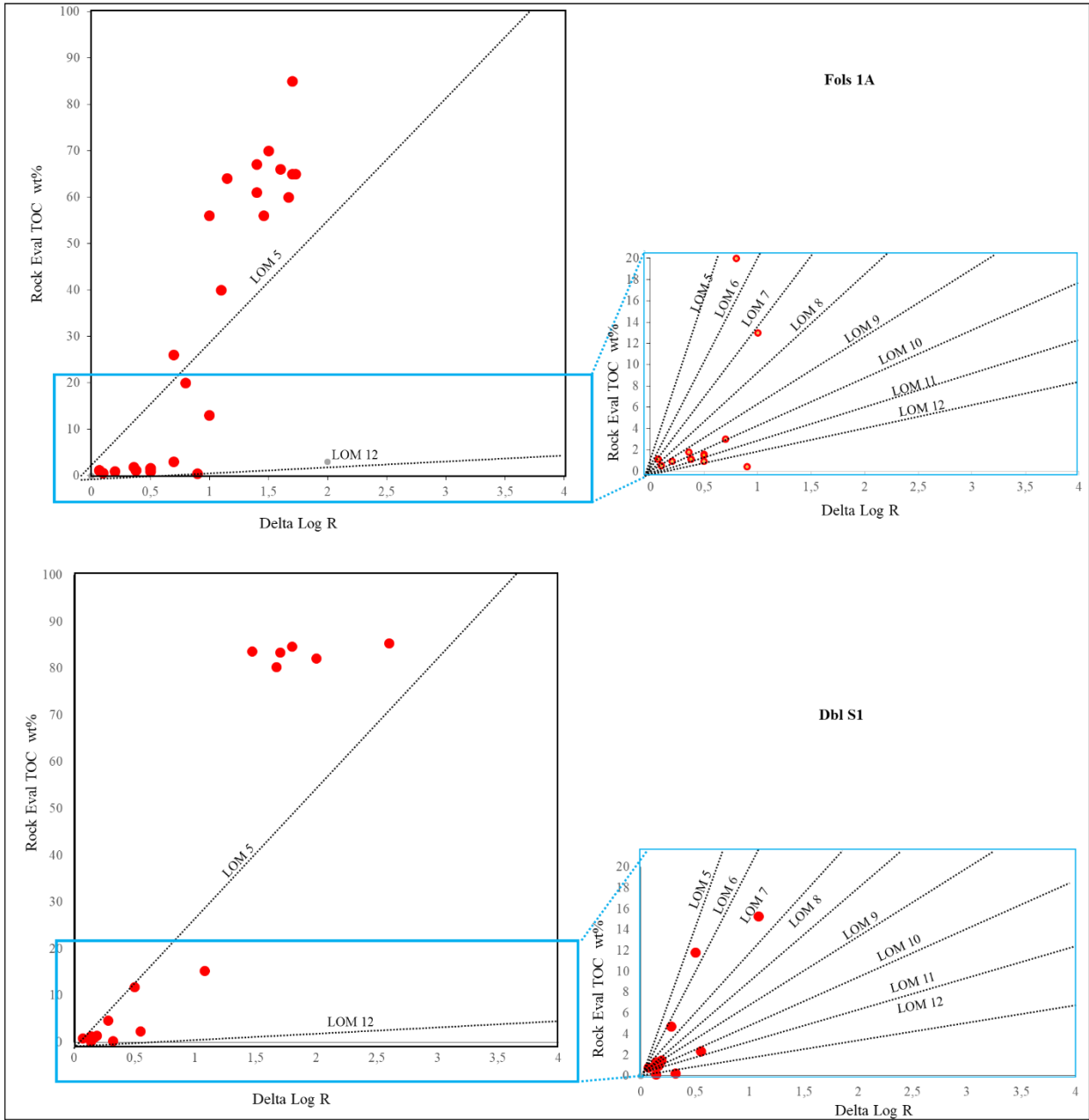
805 a function of Sonic Slowness only for coaly lithologies.



806

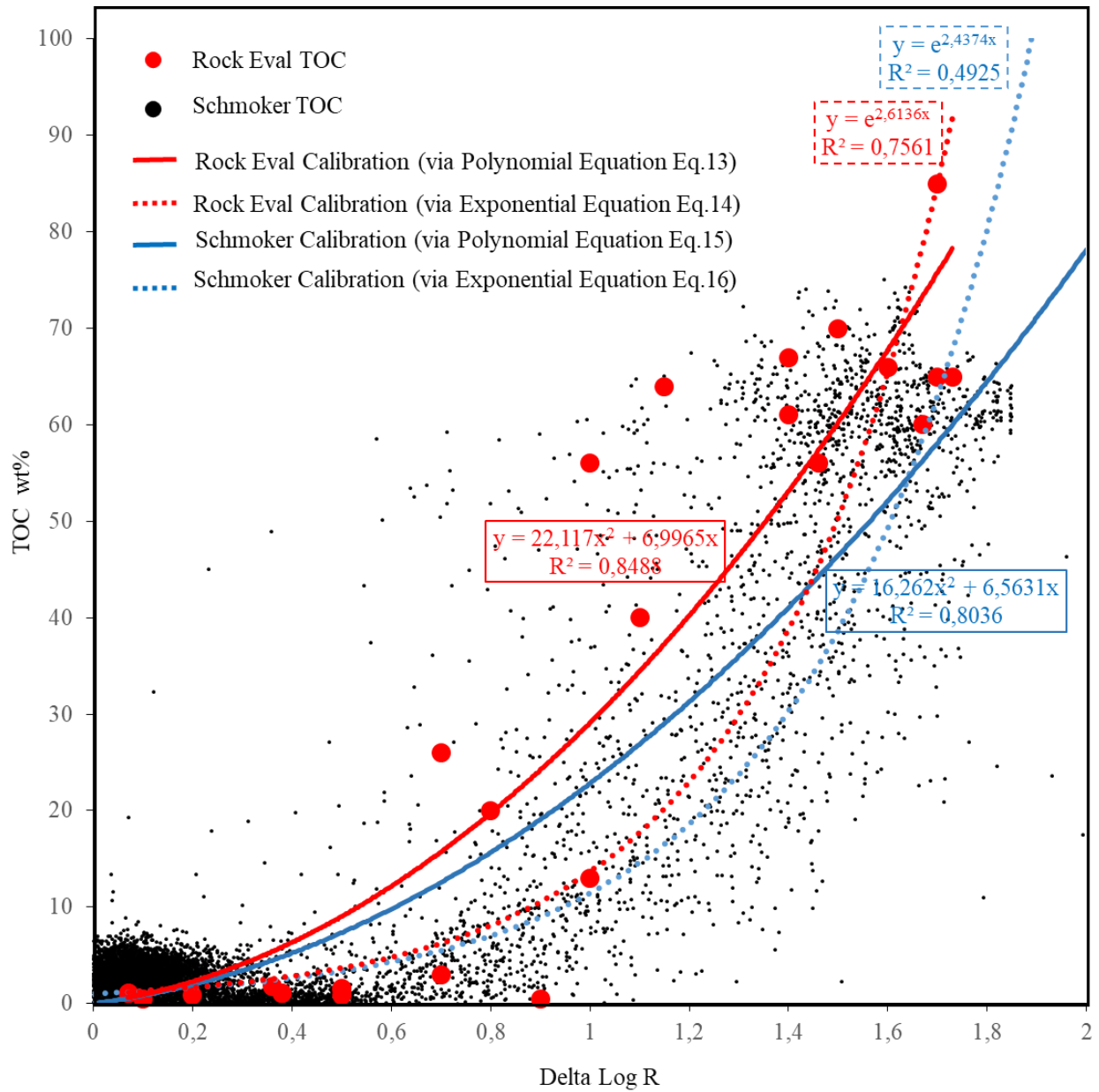
807 **Fig. 9:** Assessment of total organic carbon (TOC in wt%) in Fols 1A and Dbl S1 wells using

808 different calculation methods based on well log data as box plot analysis.



809

810 **Fig. 10:** Examining the Relationship between TOC (wt%) values and Delta log R using the diagram  
 811 of [Passey et al. \(1990\)](#) for Fols1A and Dbl S1 wells.



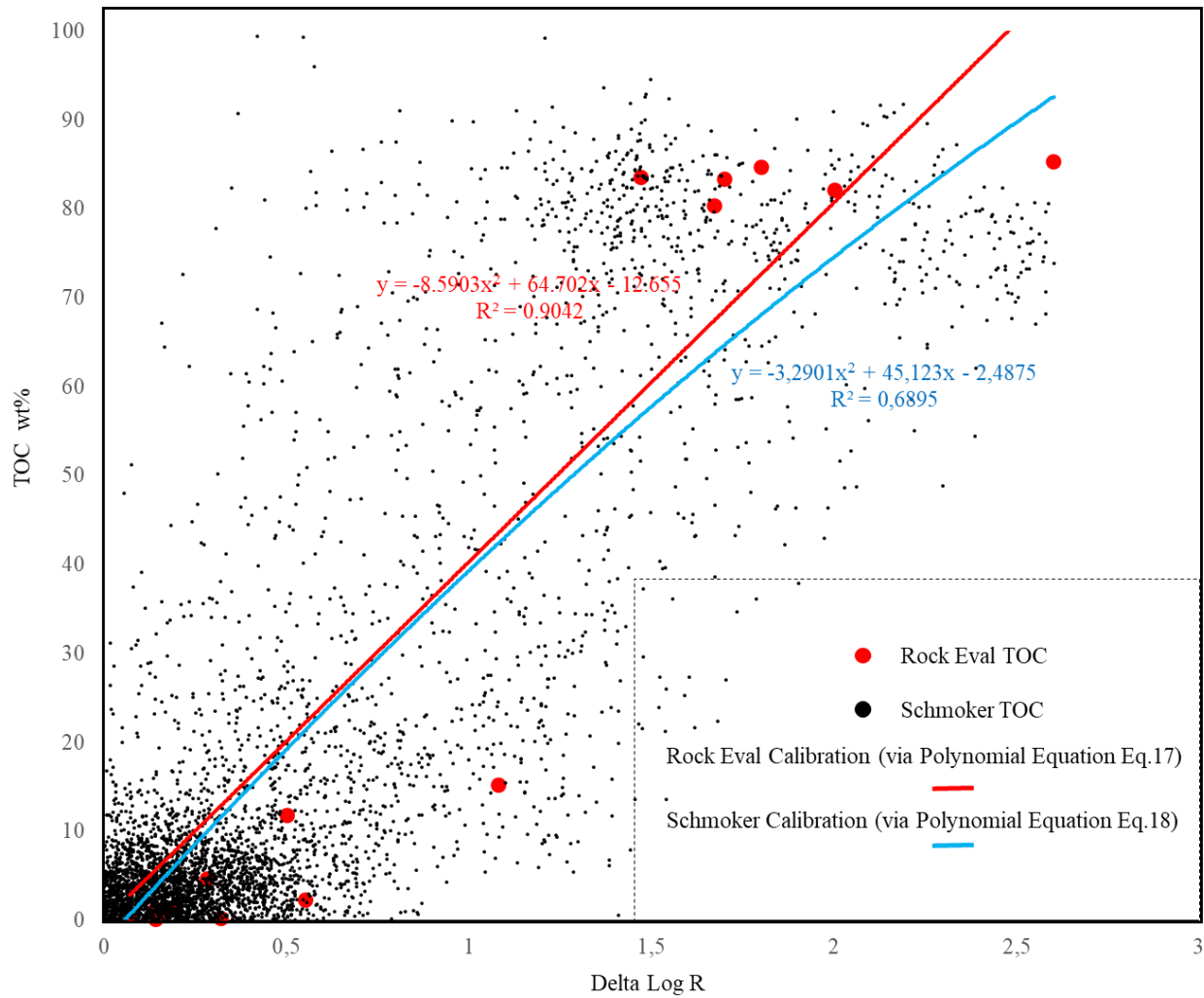
812

813 **Fig. 11:** Correlation equations between Rock-Eval measurements (red dots) and calculated using

814 [Schmoker \(1979, 1981\)](#) (black dots) TOC (wt%) versus delta log R ([Passey et al., 1990](#)) for

815 Fols 1A well using different calibration equations.

816



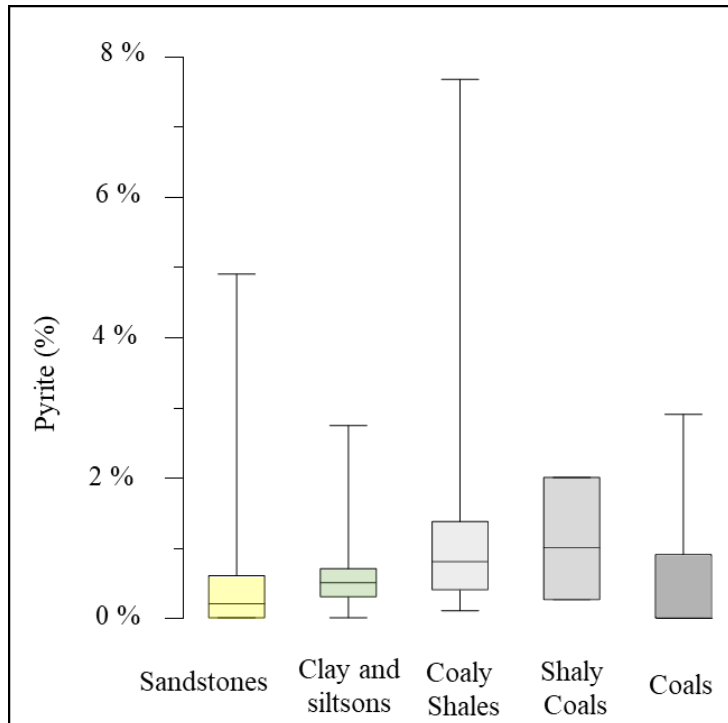
817

818 **Fig. 12:** Correlation equations between Rock-Eval measurements (red dots) and calculated using

819 [Schmoker \(1979, 1981\)](#) (black dots) TOC (wt%) versus Delta log R ([Passey et al., 1990](#)) for

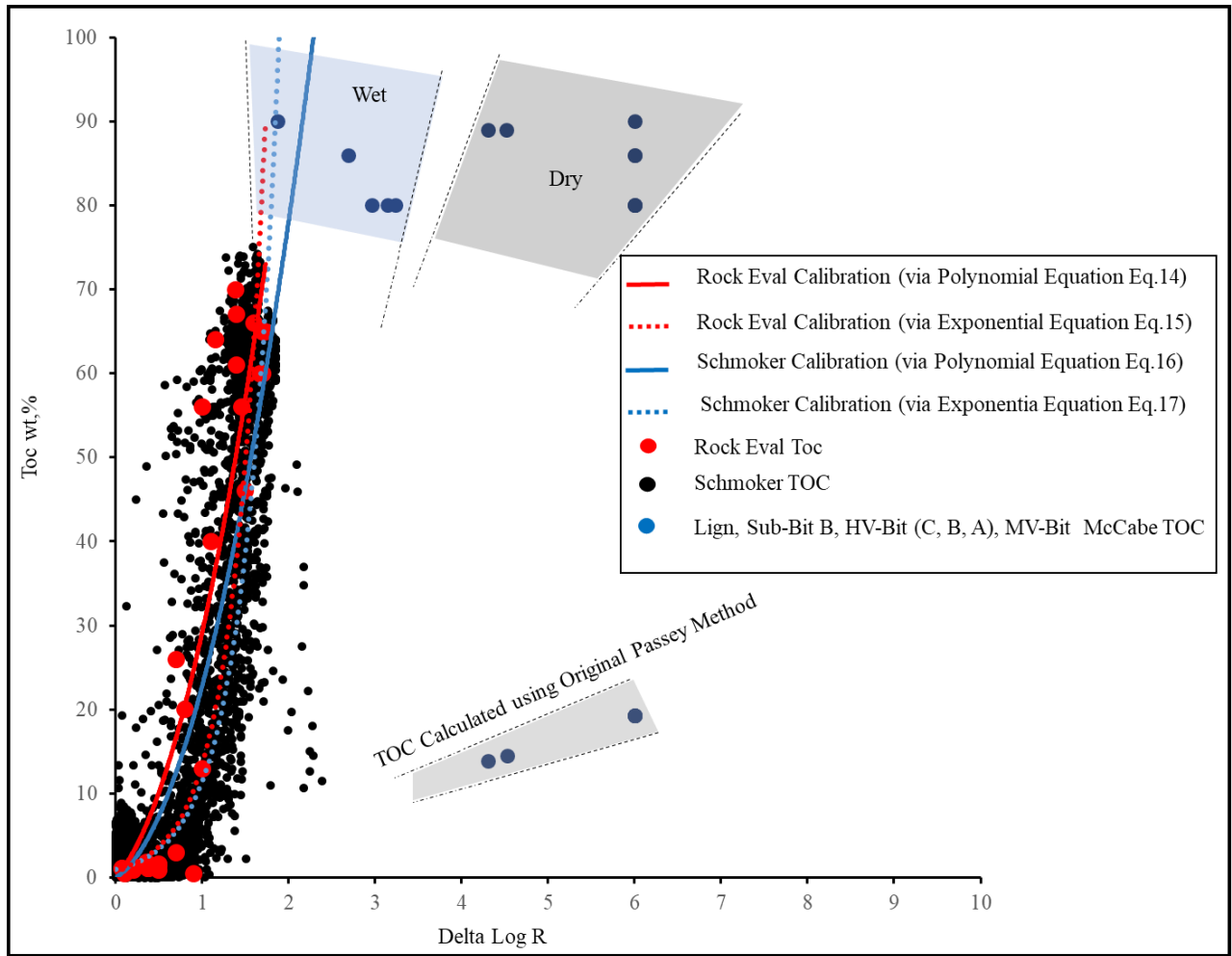
820 DBL S1 well using different calibration equations.

821



822

823 **Fig. 13:** Percentage of pyrite in different lithologies of Fols 1A and Dbl S1 wells. Data obtained  
 824 from XRD and petrographic analyses.



825

826 **Fig. 14:** Measured Rock Eval and calculated Schmoker TOC (wt%) values plotted against  
 827 Delta log R for the Fols 1A well.

828 **Tables**

829

830 **Table 1.** Vitrinite reflectance (%Ro) and Level of Organic Maturity determined after [Hood et al.](#)  
 831 [\(1975\)](#) for samples from Fols 1A and DBLS 1 wells.

Well Name	Depth MD (m)	Vitrinite reflectance (%Ro)	Level of organic maturity (LOM)
Dbl S1	1300	0.96	10.65
Fols 1A	1094	0.84	10.12
Fols 1A	1100	0.85	10.17
Fols 1A	1150	0.89	10.36
Fols 1A	1160	0.84	10.12
Fols 1A	1162	0.89	10.36
Fols 1A	1267	0.84	10.12
Fols 1A	1286	0.93	10.53

832  
 833  
 834  
 835  
 836

**Table 2.** Delta log R Baseline values used for TOC calculations.

Well Name	Baseline Values	
	Resistivity (Ohm.m)	Sonic slowness ( $\mu$ s/ft)
Fols 1A	150	65
Dbl S1	100	80

837

838 **Table 3.** Table of resistivity data as a function of coal rank and TOC values for different coal types:  
839 Resistivity data as a function of coal rank and TOC values for different coal types. The resistivity  
840 values for bituminous coal (Max and Min) ([Telford et al., 1990](#)), while the resistivity values for  
841 sub-bituminous coal B and medium- and high-volatile bituminous coal (C, B and A) were derived  
842 from the reference data study of [McCabe and Tholey. \(1945\)](#) .TOC values for each coal type were  
843 based on the Passey equation and Rock Eval TOC values as reported by [Mastalerz et al. \(2011\)](#) (  
844 <sup>1</sup>The wet coal samples were impregnated in water for 24 hours before being subjected to resistivity  
845 measurement after [McCabe and Tholey. \(1945\)](#) ).

846

Rank	Resistivity (ohm.m)		Delta log R		Passey TOC (wt%)		Expected TOC (wt%)
	Dry	Wet <sup>1</sup>	Dry	Wet <sup>1</sup>	Dry	Wet <sup>1</sup>	
Sub-bituminous B Coal	3.10 <sup>6</sup>	5100	6	3.23	19.32	10.40	-
High volatile C bituminous Coal (1)	3.10 <sup>6</sup>	2740	6	2.96	19.32	9.53	80
High volatile C bituminous Coal (2)	3.10 <sup>6</sup>	4150	6	3.14	19.32	10.11	80
High volatile B bituminous Coal	3.10 <sup>6</sup>	ND	6	ND	19.32	ND	86
High volatile A bituminous Coal	3.10 <sup>6</sup>	1480	6	2.69	19.32	8.67	86
Medium volatile bituminous Coal	3.10 <sup>6</sup>	220	6	1.87	19.32	6	90
Bituminous Coal (Max )	10 <sup>5</sup>	ND	4.52	ND	14.56	ND	89
Bituminous Coal (Min )	6.10 <sup>4</sup>	ND	4.30	ND	13.85	ND	89

847

848 **Table 4.** Equations used in the calculation of TOC for the Fols 1A well. R<sup>2</sup>: determination  
 849 coefficient for each method. RMSE: Root Mean Squared Error for each method compared to TOC  
 850 values obtained using the method by [Schmoker \(1979, 1981\)](#).

Methods Calibration		Eq	Modified TOC Equations	R <sup>2</sup>	RMSE (wt. %)
TOC Schmoker/Passey Ratio		11	$TOC = \Delta \text{Log } R * 10^{(2.297-0.1688*LOM)} * (19.15 * \ln(\Delta T) - 83.48)$	<b>0.82</b>	<b>8.52</b>
(Delta log R separation) Vs (TOC Calibration)	With Rock Eval TOC	13	$TOC = 22.117 * \Delta \text{Log } R^2 + 6.997 * \Delta \text{Log } R$	0.79	9.12
		14	$TOC = e^{2.6136*\Delta \text{Log } R}$	0.58	14
	With Schmoker TOC	15	$TOC = 16.262 * \Delta \text{Log } R^2 + 6.5631 * \Delta \text{Log } R$	0.79	7.04
		16	$TOC = e^{2.4374*\Delta \text{Log } R}$	0.62	5.23
Multivariate regression		19	$TOC = 0.73 * \Delta t - 0.065 * \text{GammaRay} + 0.02 * R - 46.29$	<b>0.82</b>	<b>6.6</b>

851  
 852  
 853 **Table 5.** Equations used in the calculation of TOC for the Dbl S1. R<sup>2</sup>: determination coefficient  
 854 for each method. RMSE, Root Mean Squared Error for each method compared to TOC values  
 855 obtained using the method by [Schmoker \(1979, 1981\)](#).  
 856

Methods Calibration		Eq	Modified TOC Equations	R <sup>2</sup>	RMSE (wt. %)
TOC Schmoker/Passey Ratio		12	$TOC = \Delta \text{Log } R * 10^{(2.297-0.1688*LOM)} * (23.298 * \ln(\Delta T) - 103.48)$	<b>0.76</b>	<b>12</b>
(Delta log R separation) Vs (TOC Calibration)	With Rock Eval TOC	17	$TOC = - 8.5903 * \Delta \text{Log } R^2 + 64.702 * \Delta \text{Log } R - 12.655$	0.62	17
	With Schmoker TOC	18	$TOC = - 3.2901 * \Delta \text{Log } R^2 + 45.123 * \Delta \text{Log } R - 2.4875$	0.64	12
Multivariate regression		20	$TOC = 0.82 * \Delta t - 0.066 * \text{GammaRay} + 0.02 * R - 64.15$	<b>0.73</b>	<b>9.7</b>

857